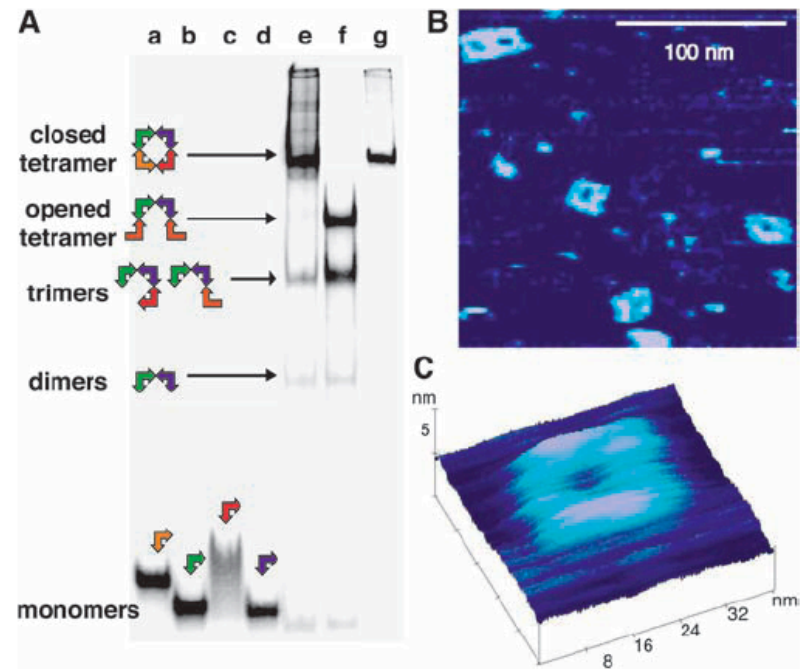
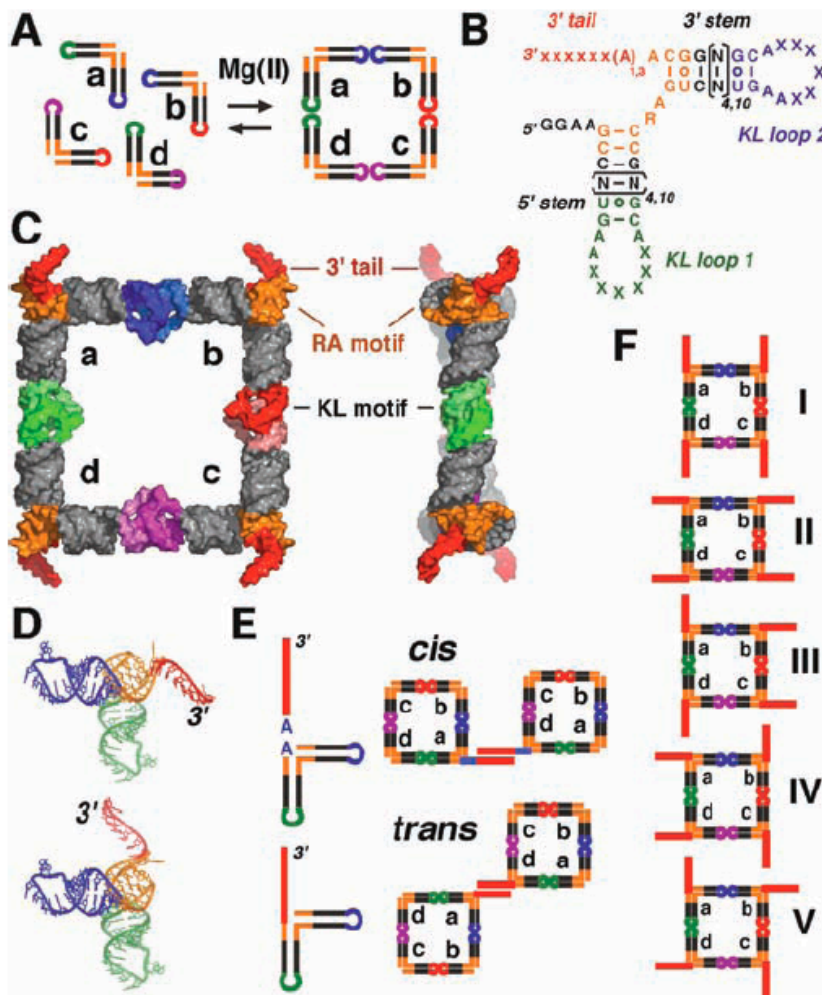


RNA Self-assembly

Building Programmable Jigsaw Puzzles with RNA

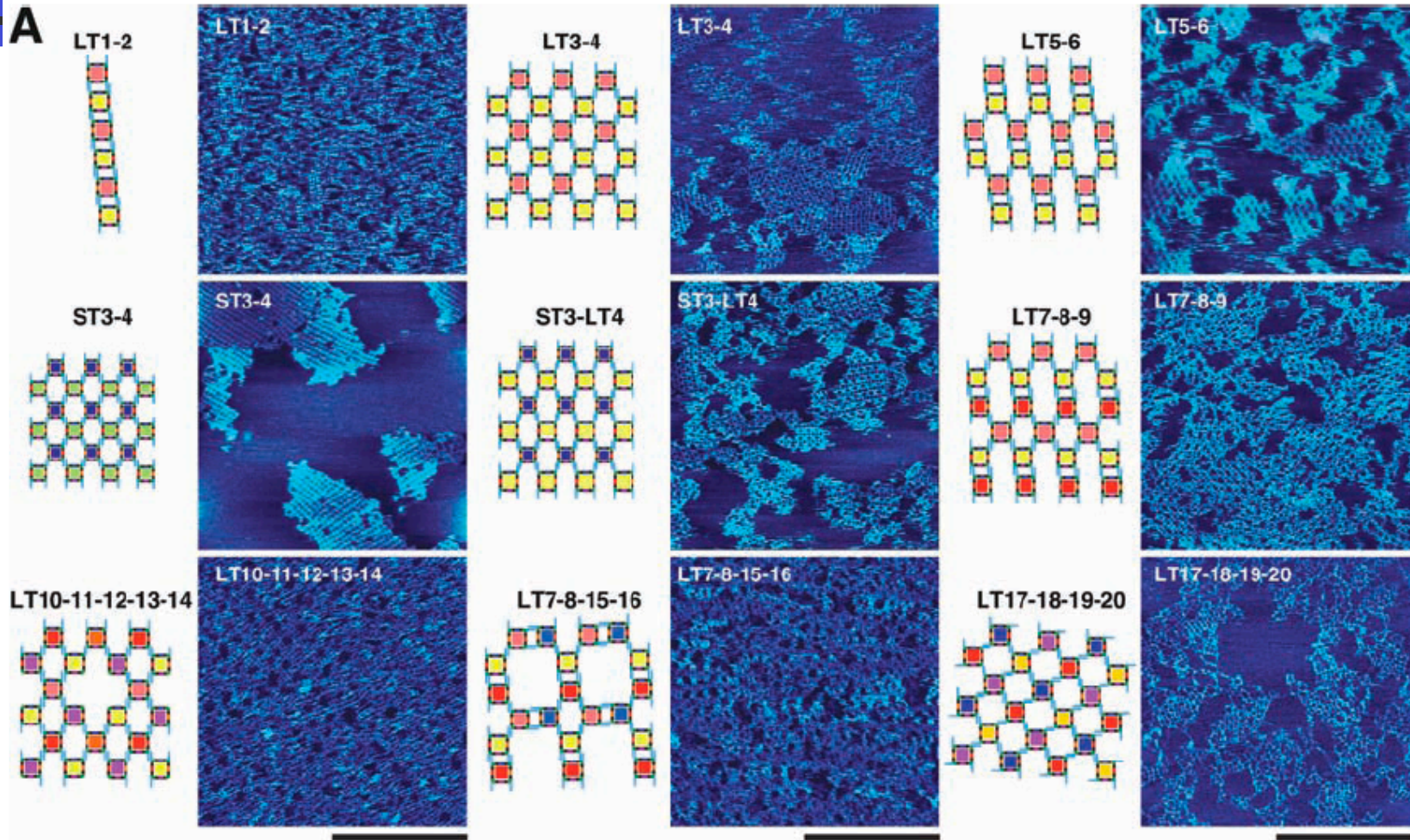
Arkadiusz Chworos,¹ Isil Severcan,¹ Alexey Y. Koyfman,^{1,2}
Patrick Weinkam,^{1,4} Emin Oroudjev,³ Helen G. Hansma,³
Luc Jaeger^{1,2*}

(2004) *Science* **306**, 2068-2072



RNA Self-assembly

(2004) *Science* **306**, 2068-2072

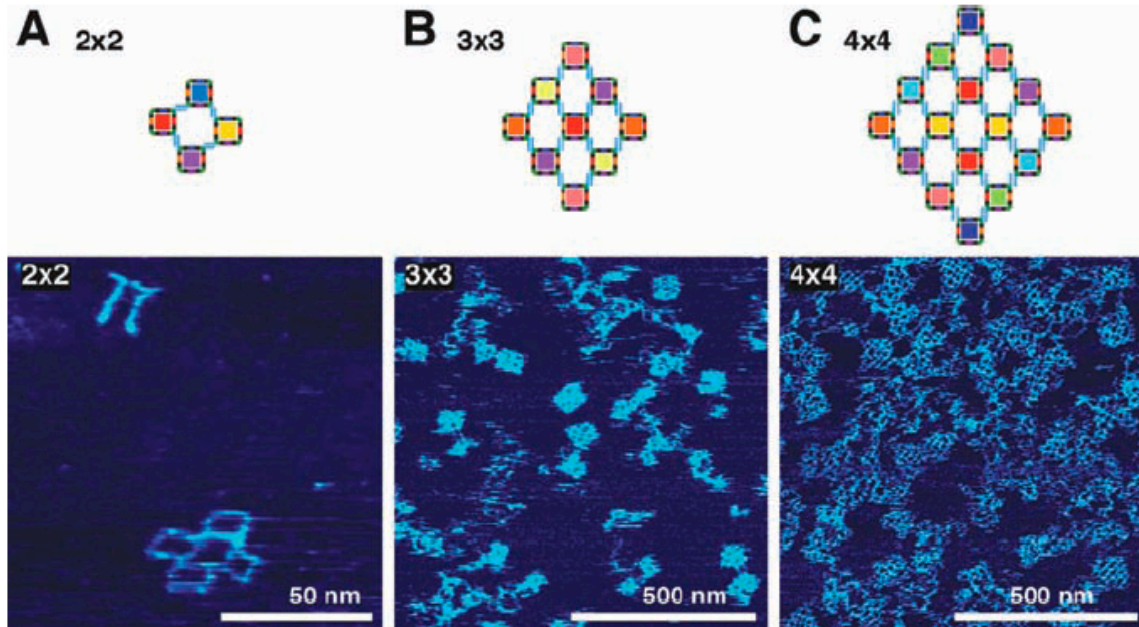
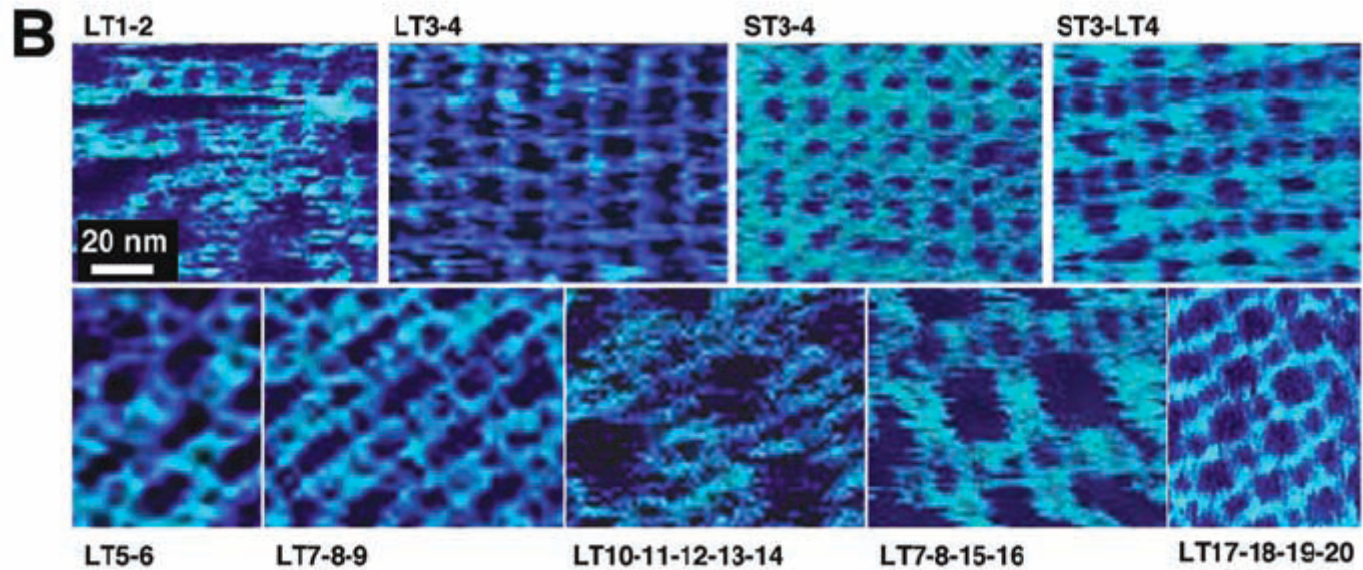
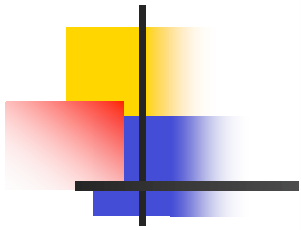


3/29/06

LaBean COMPSCI 296.5

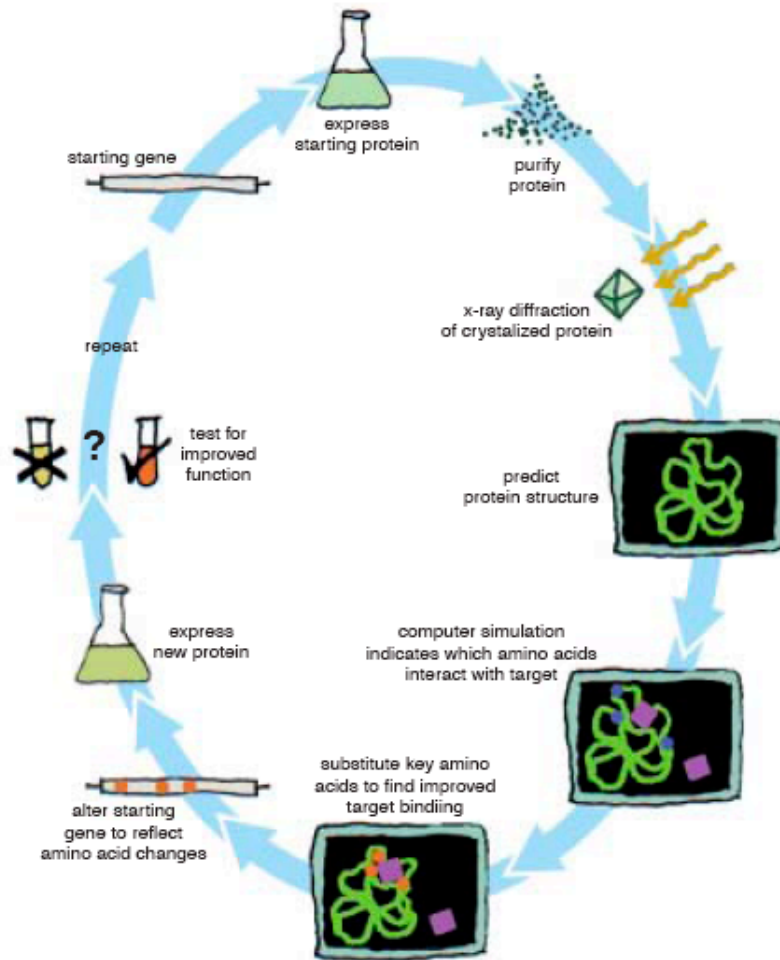
RNA Self-assembly

(2004) *Science* **306**, 2068-2072

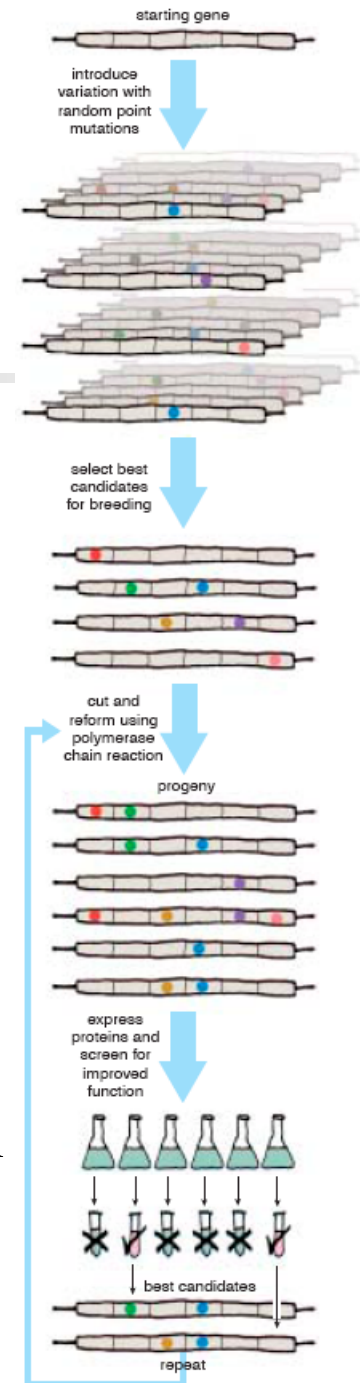


3/29/06

2003



Rational design



Directed evolution

3/29/06

LaBean COMPSCI 296.5

RNA Physical Catalyst

RNA-Mediated Metal-Metal Bond Formation in the Synthesis of Hexagonal Palladium Nanoparticles

Lina A. Gugliotti, Daniel L. Feldheim,* Bruce E. Eaton*
(2004) *Science* 304, 850-852

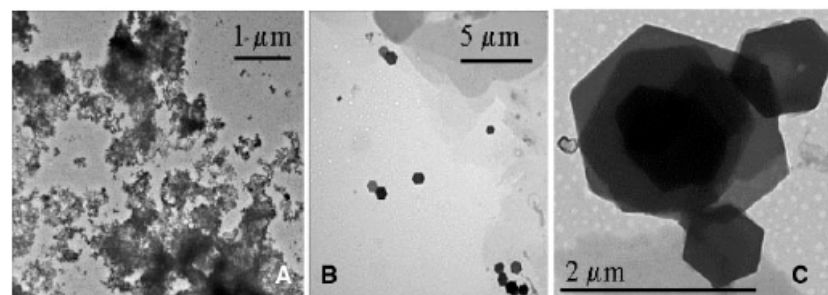
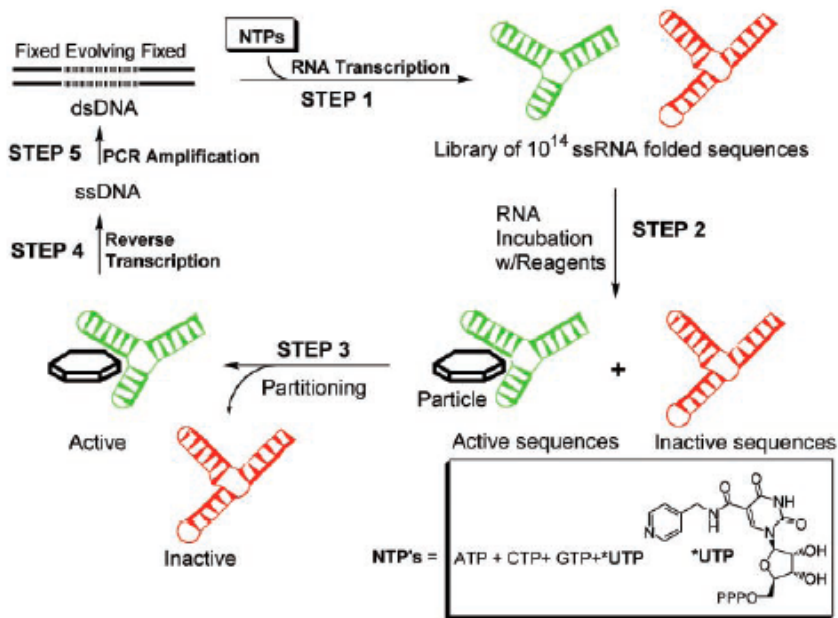


Fig. 1. Transmission electron micrograph images of palladium particles formed in the presence of cycle 0 pool modified RNA (A) and the cycle 8 RNA pool (B and C).

| | |
|---|---|
| <p>Family 1 (14 members, 56%)</p> <p>PD_017 5'-CCUUCUUAUCCU CAAGG ACCAACA AAAAAUGUA JUCC-3'</p> <p>PD_021 5'-CUUCUUAUCCUCAAAGUACCAACU AAAAAUGUA GCCC-3'</p> <p>PD_024 5'-CCUUCUUAUCCU CAAGG ACCAACU AAAAAUGUA JUCC-3'</p> <p>PD_025 5'-CCUUCUUAUCCU CAAGG ACCAACU AAAAAUGUA JUCC-3'</p> <p>PD_028 5'-CCUUCUUAUCCU CAAGG ACCAACA AAAAAUGUA JUCC-3'</p> <p>PD_029 5'-CCUUCUUAUCCU CAAGG ACCAACA AAAAAUGUA JUCC-3'</p> <p>PD_031 5'-CCUUCUUAUCCU CAAGG ACCAACA AAAAAUGUA JUCC-3'</p> <p>PD_032 5'-CCUUCUUAUCCU CAAGG ACCAACA AAAAAUGUA JUCC-3'</p> <p>PD_062 5'-CCUUCUUAUCCU CAAGG ACCAACA AAAAAUGUA JUCC-3'</p> <p>PD_085 5'-CCUUCUUAUCCU CAAGG ACCAACU AAAAAUGUA JUCC-3'</p> <p>PD_086 5'-CCUUCUUAUCCU CAAGG ACCAACU AAAAAUGUA JUCC-3'</p> <p>PD_090 5'-CCUUCUUAUCCU CAAGG ACCAACU AAAAAUGUA JUCC-3'</p> <p>PD_093 5'-CCUUCUUAUCCU CAAGG ACCAACA AAAAAUGUA JUCC-3'</p> <p>PD_094 5'-CCUUCUUAUCCU CAAGG ACCAACA AAAAAUGUA JUCC-3'</p> | <p>Family 2 (6 members, 24%)</p> <p>PD_019 5'-CUCCUUAUACCUCAA AAUACCCCAUCLU UAGUACGUUA-3'</p> <p>PD_022 5'-CUCCUUAUACCUUUA AAUACCCCAUCLU UAGUACGUUA-3'</p> <p>PD_026 5'-CUCCUUAUACCUUUA AAUACCCCAUCLU UAGUACGUUA-3'</p> <p>PD_027 5'-CUCCUUAUACCUUUA AAUACCCCAUCLU UAGUACGUUA-3'</p> <p>PD_030 5'-CUCCUUAUACCUUUA AAUACCCCAUCLU UAGUACGUUA-3'</p> <p>PD_092 5'-CUCCUUAUACCUUUA AAUACCCCAUCLU UAGUACGUUA-3'</p> |
| <p>Family 3 (2 members, 8%)</p> <p>PD_020 5'-CUCCUUAUACCUUUA AAUACCCCAUCLU UAGUACGUUA-3'</p> <p>PD_091 5'-CUCCUUAUACCUUUA AAUACCCCAUCLU UAGUACGUUA-3'</p> | <p>Family 4 (2 members, 8%)</p> <p>PD_081 5'-CCUUCUUAUACCUUUA AAUACCCCAUCLU UAGUACGUUA-3'</p> <p>PD_089 5'-CCUUCUUAUACCUUUA AAUACCCCAUCLU UAGUACGUUA-3'</p> |
| <p>Orphan</p> <p>PD_084 5'-CCUUCUUAUACCUUUA AAUACCCCAUCLU UAGUACGUUA-3'</p> | |

*UTP is 5-(4-pyridylmethyl)-uridine 5' triphosphate
Pd₂(DBA)₃ is dibenzylidene-acetone palladium (0)

RNA Physical Catalyst

RNA-Mediated Control of Metal Nanoparticle Shape

Lina A. Gugliotti,[†] Daniel L. Feldheim,^{*,†} and Bruce E. Eaton^{*,†,‡}

J. AM. CHEM. SOC. 2005, 127, 17814–17818

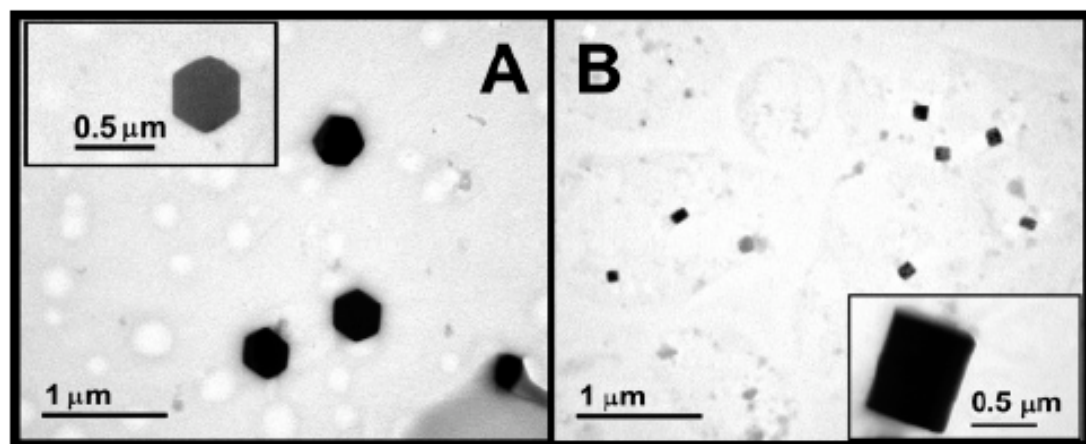


Figure 2. TEM micrographs of (A) hexagonal palladium particles formed in the presence of Pdase 17 and (B) cubic palladium particles formed in the presence of Pdase 34.

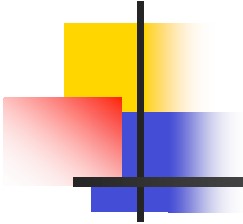
Table 1. Metal Precursor Effects on Particle Shape and Size

| RNA isolate | metal precursor | particle shape | size (μm) | % population |
|-----------------------------|-----------------------------|-------------------|------------------------|--------------|
| 17 | $\text{Pd}_2(\text{DBA})_3$ | hexagonal | 1.24 ± 0.57 | 100 |
| | | spherical | 0.10 ± 0.06 | 14 |
| | $\text{Pt}_2(\text{DBA})_3$ | cubic | 0.22 ± 0.13 | 16 |
| | | hexagonal | 0.46 ± 0.22 | 69 |
| | | spherical | 0.27 ± 0.16 | 100 |
| 34 | $\text{Pd}_2(\text{DBA})_3$ | spherical | 0.007 ± 0.003 | 100 |
| | | hexagonal | 0.27 ± 0.10 | 100 |
| | $\text{Pt}_2(\text{DBA})_3$ | cubic | 0.10 ± 0.05 | 100 |
| | | spherical | 0.16 ± 0.05 | 2 |
| | | cubic | 0.14 ± 0.07 | 29 |
| $\text{Ni}(\text{PPh}_3)_4$ | hexagonal | 0.37 ± 0.16 | 68 | |
| | spherical | 0.31 ± 0.29 | 100 | |
| | spherical | 0.009 ± 0.007 | 100 | |
| | $\text{Ni}(\text{PPh}_3)_4$ | spherical | 0.24 ± 0.10 | 100 |

*UTP is 5-(4-pyridylmethyl)-uridine 5' triphosphate

$\text{Pd}_2(\text{DBA})_3$ is dibenzylidene-acetone palladium (0)

Ellington & Szostak



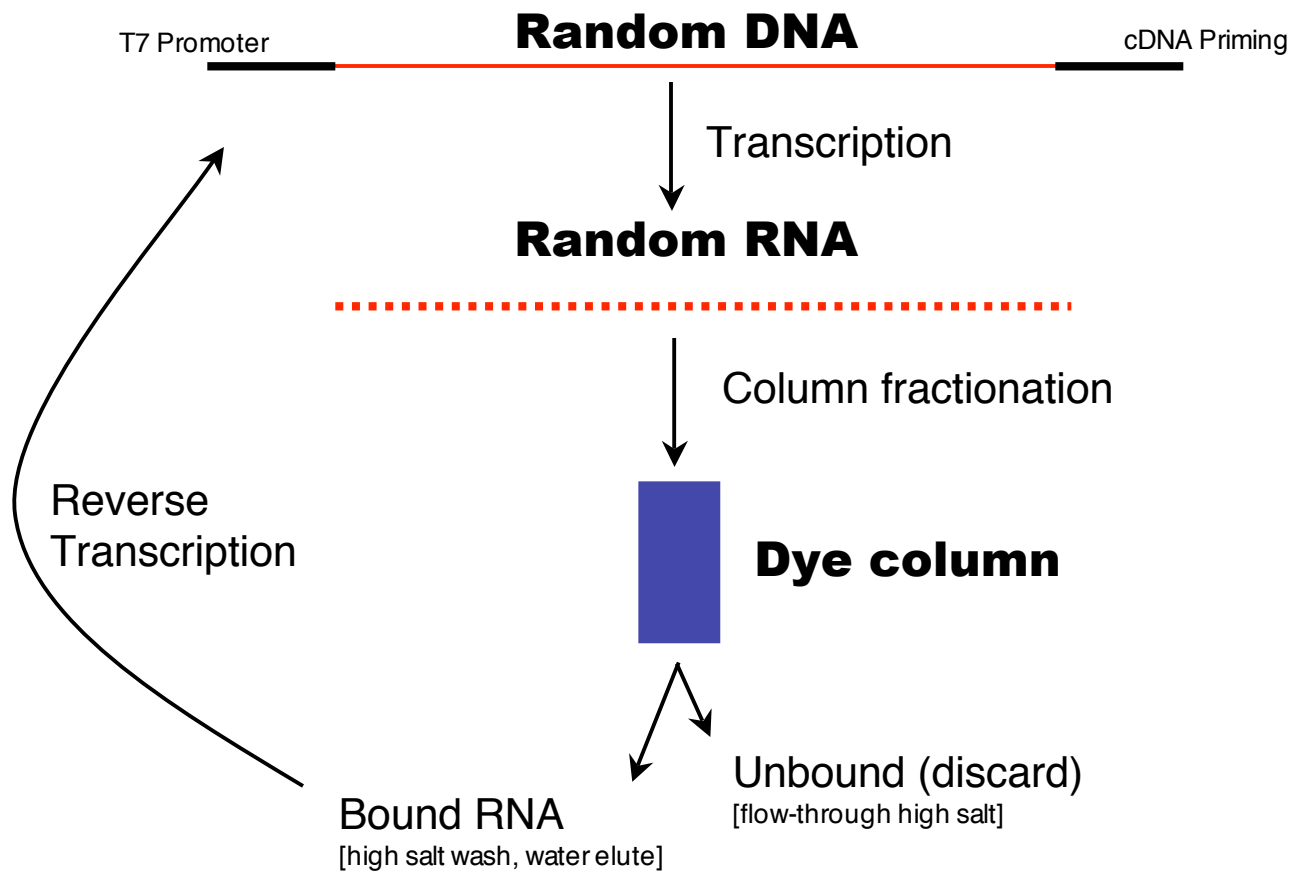
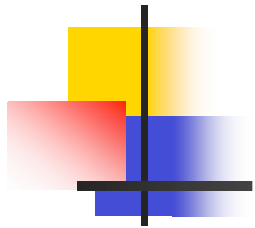
Nature. 1990 Aug 30;346(6287):818-22.

In vitro selection of RNA molecules that bind specific ligands.

Ellington AD, Szostak JW.

Department of Molecular Biology, Massachusetts General Hospital, Boston 02114.

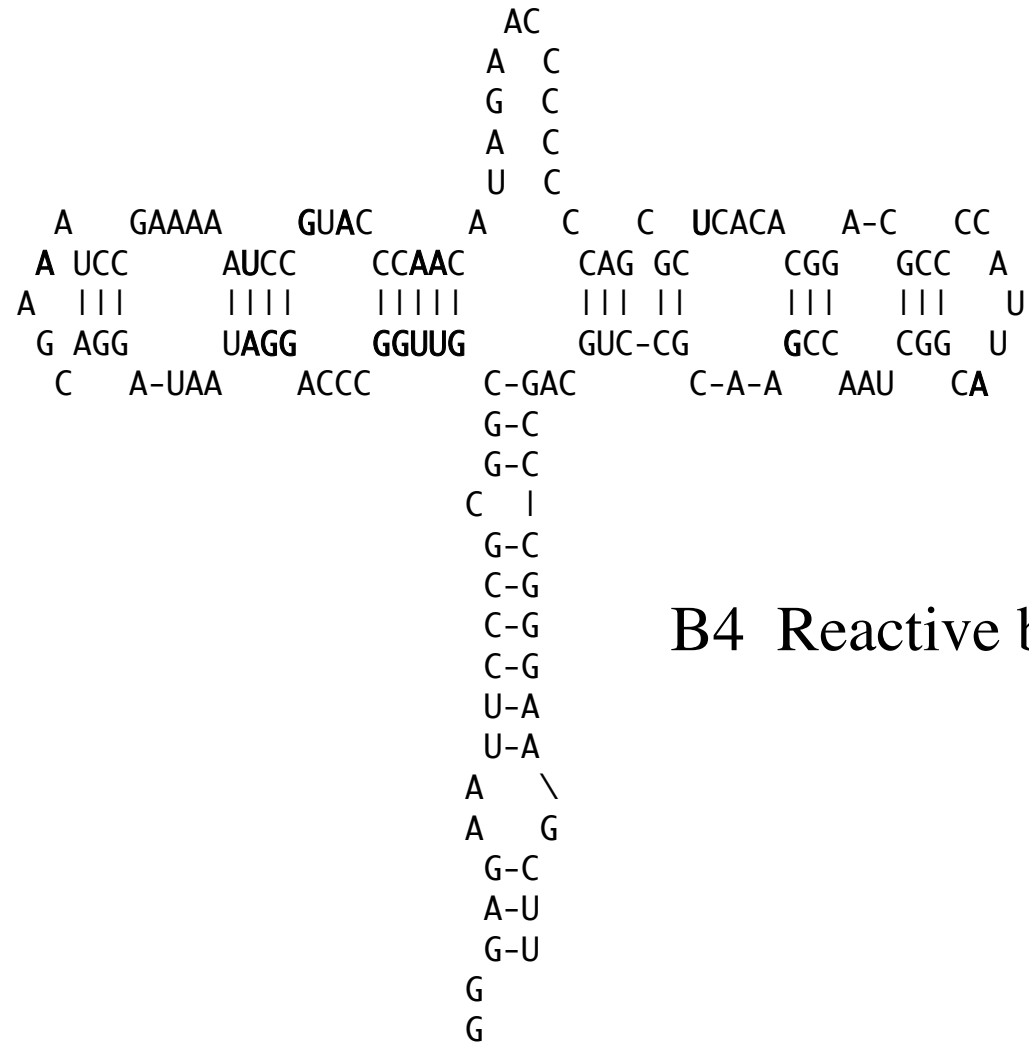
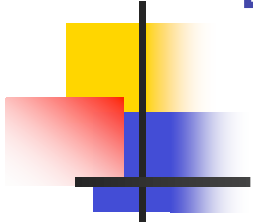
Subpopulations of RNA molecules that bind specifically to a variety of organic dyes have been isolated from a population of random sequence RNA molecules. Roughly one in 10^{10} random sequence RNA molecules folds in such a way as to create a specific binding site for small ligands.



- 100 random nucleotides (+ constant regions)
- Complexity of initial pool $\sim 10^{15}$ (10^{60} possible)
- Poor transcription; PCR amp; $\sim 10^{13}$ diversity
- $\sim 4 \times 10^{14}$ RNA molecules applied to column
- $< 0.1\%$ of initial RNA library bound then after 4 to 5 cycles of bind, RT, PCR, Transcribe, rebind $\sim 50\%$ of RNA molecules bound.
- Binding is specific for dye selected.
- For 1 column 20 clones were sequenced ~ 16 -20 nucleotides were invariant over the set of clones.
- APTAMER from Latin 'aptus', to fit.

Ellington & Szostak

Nature. 1990 Aug 30;346(6287):818-22.



B4 Reactive blue binder

Systematic Evolution of Ligands by Exponential Enrichment: RNA Ligands to Bacteriophage T4 DNA Polymerase

CRAIG TUERK AND LARRY GOLD

Science, New Series, Vol. 249, No. 4968 (Aug. 3, 1990), 505-510.

- SELEX- systematic evolution of ligands by exponential enrichment.
- Selected RNA for binding to T4 DNA polymerase.
- 65,536 possible sequences.
- Wild-type T4 bacteriophage mRNA sequence found and a variant with 50% identity to wild-type.

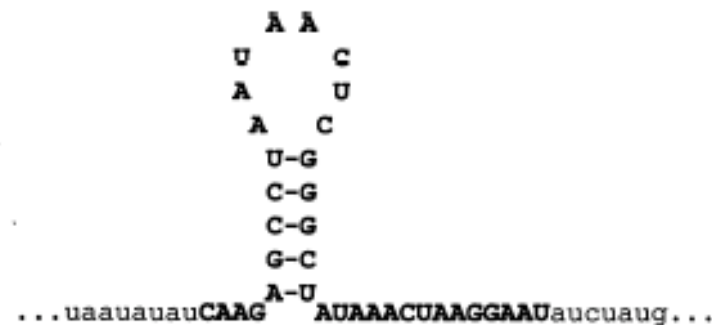
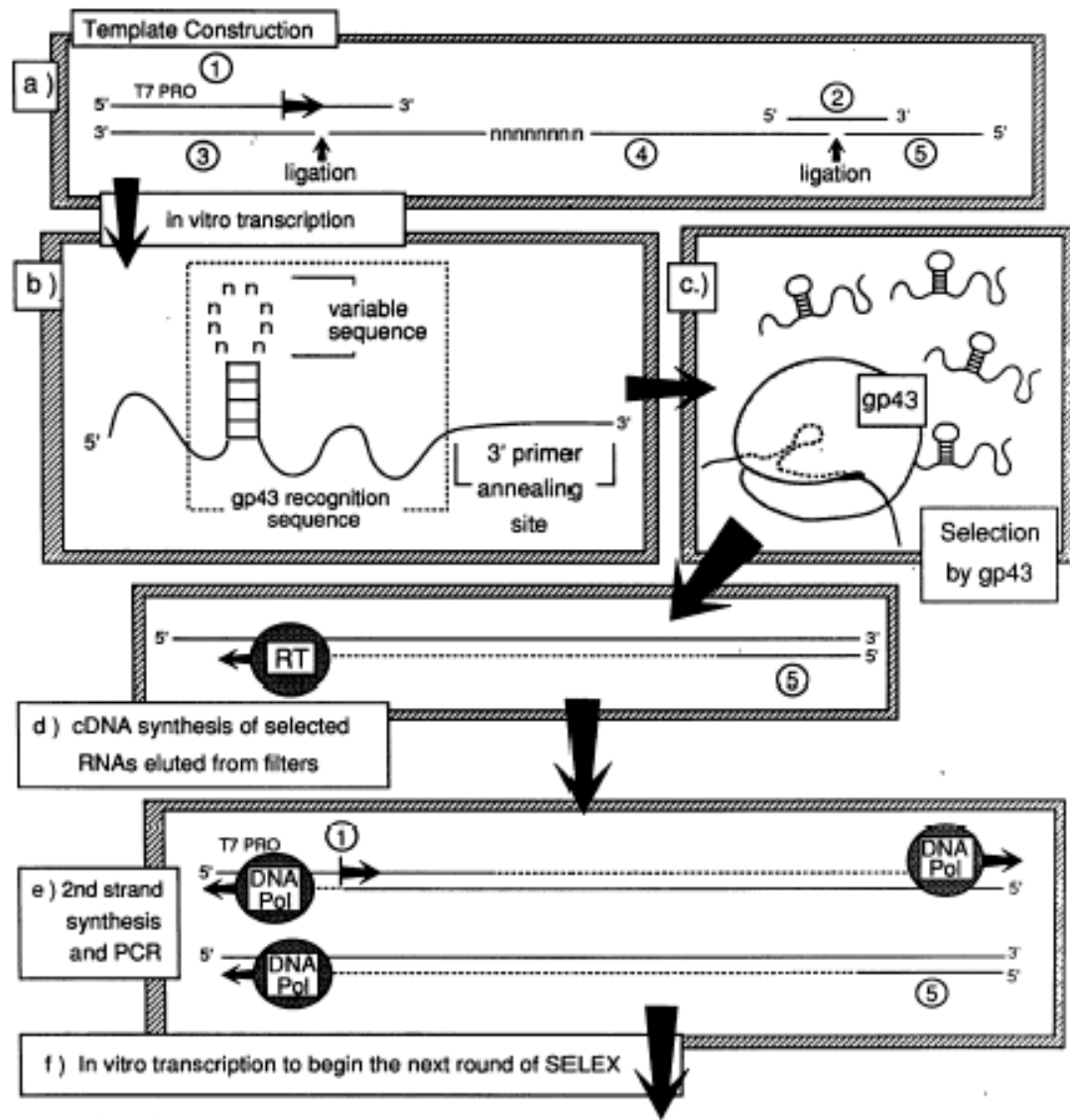
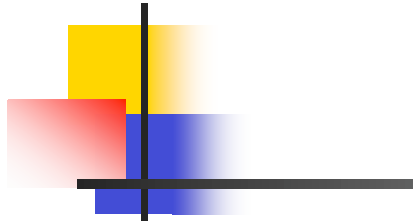


Fig. 1. The gene 43 translational operator in bacteriophage T4. Shown is the sequence at the ribosome binding site of gene 43. The bold-faced capitalized letters indicate the extent of the information required for binding of gp43 (6).



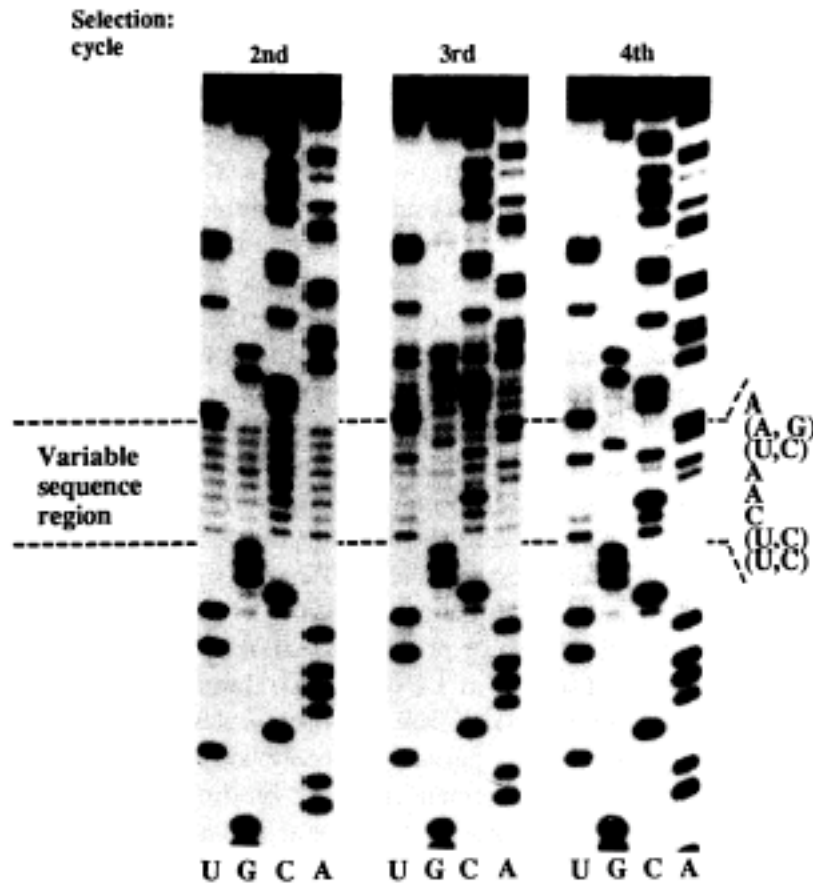


Fig. 4. Batch RNA sequences through rounds of selection. Sequencing and labeling were done as in Fig. 3. The transcripts were derived from amplified products of selections 2, 3, and 4 for experiment B.

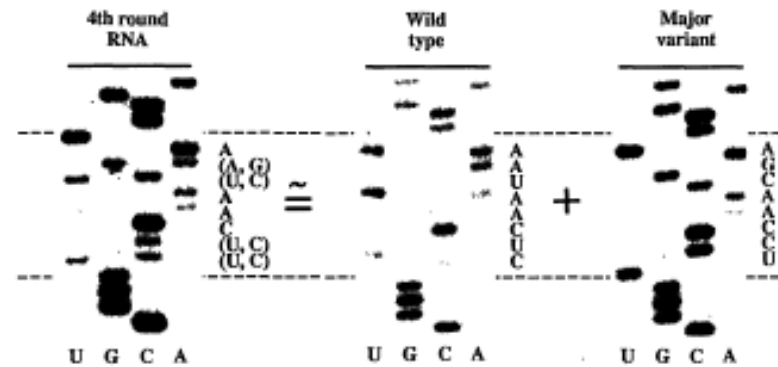


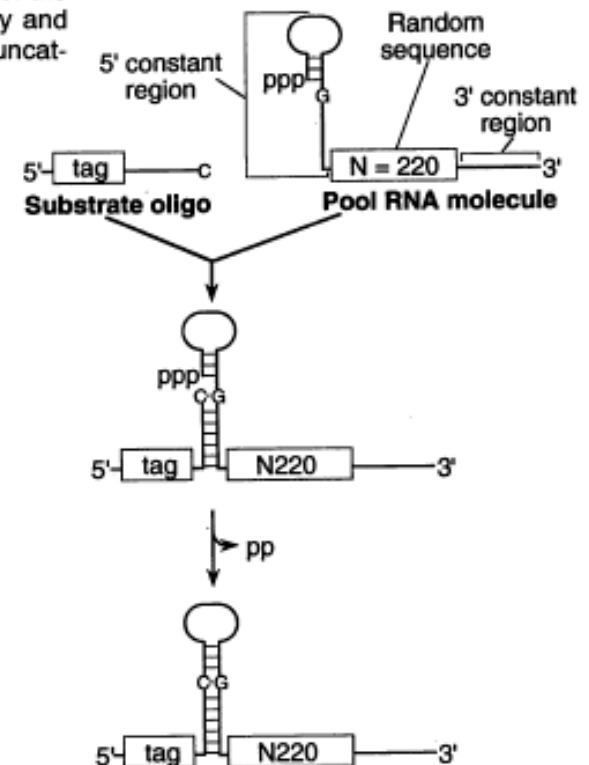
Fig. 6. The clonal composition of the "consensus" sequence. Of the three sequencing gels, the first is the batch sequencing of selected RNA's as shown in Fig. 4 for experiment B; the second and third gels show sequencing products derived from plasmid templates (26) of representative clonal isolates of the batch population. These two individual sequences alone yield the batch "consensus" that is observed.

Isolation of New Ribozymes from a Large Pool of Random Sequences

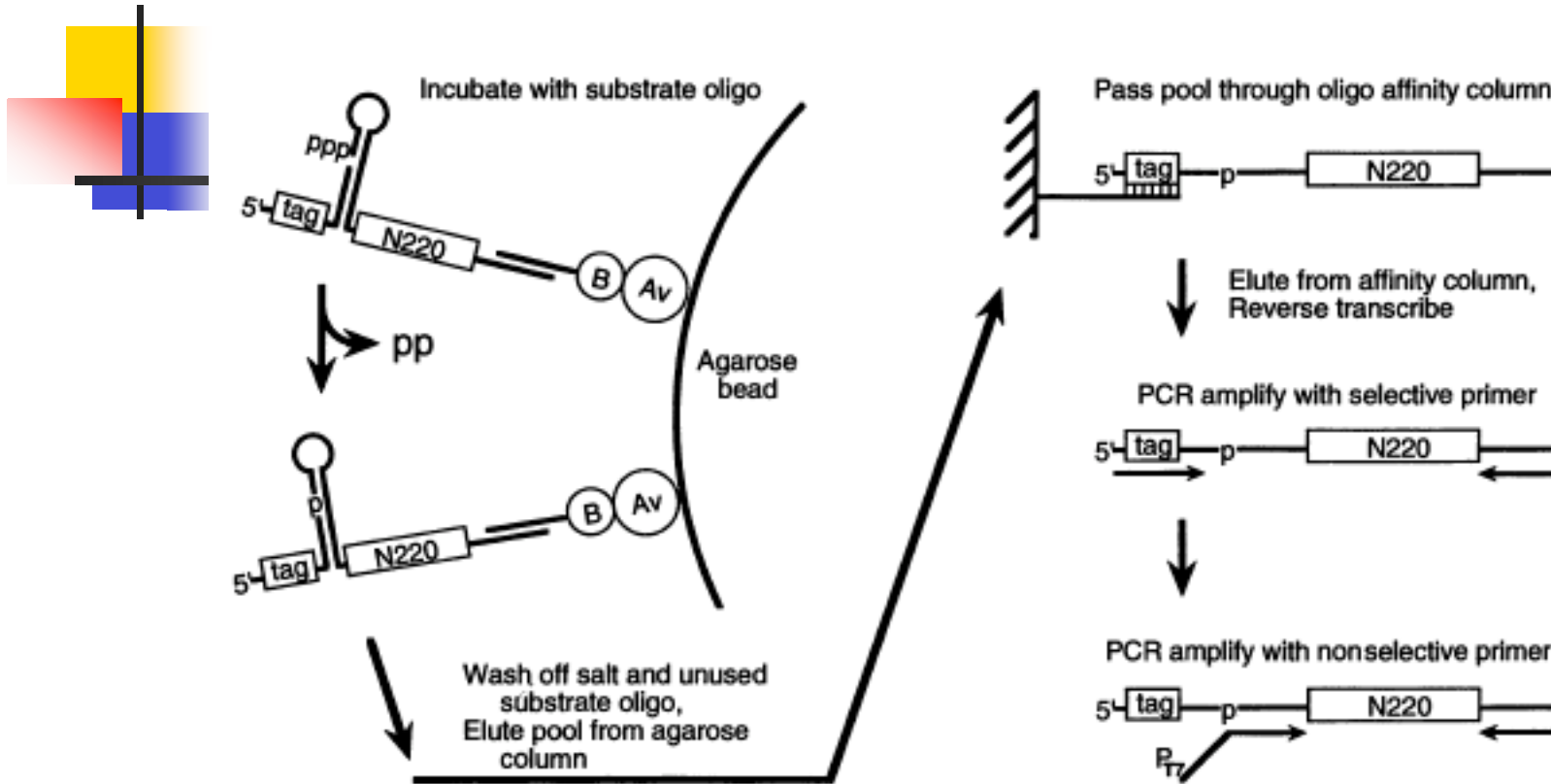
David P. Bartel and Jack W. Szostak

An iterative in vitro selection procedure was used to isolate a new class of catalytic RNAs (ribozymes) from a large pool of random-sequence RNA molecules. These ribozymes ligate two RNA molecules that are aligned on a template by catalyzing the attack of a 3'-hydroxyl on an adjacent 5'-triphosphate—a reaction similar to that employed by the familiar protein enzymes that synthesize RNA. The corresponding uncatalyzed reaction also yields a 3',5'-phosphodiester bond. In vitro evolution of the population of new ribozymes led to improvement of the average ligation activity and the emergence of ribozymes with reaction rates 7 million times faster than the uncatalyzed reaction rate.

- 220 random positions
- 1.6×10^{15} diversity



Bartel & Szostak

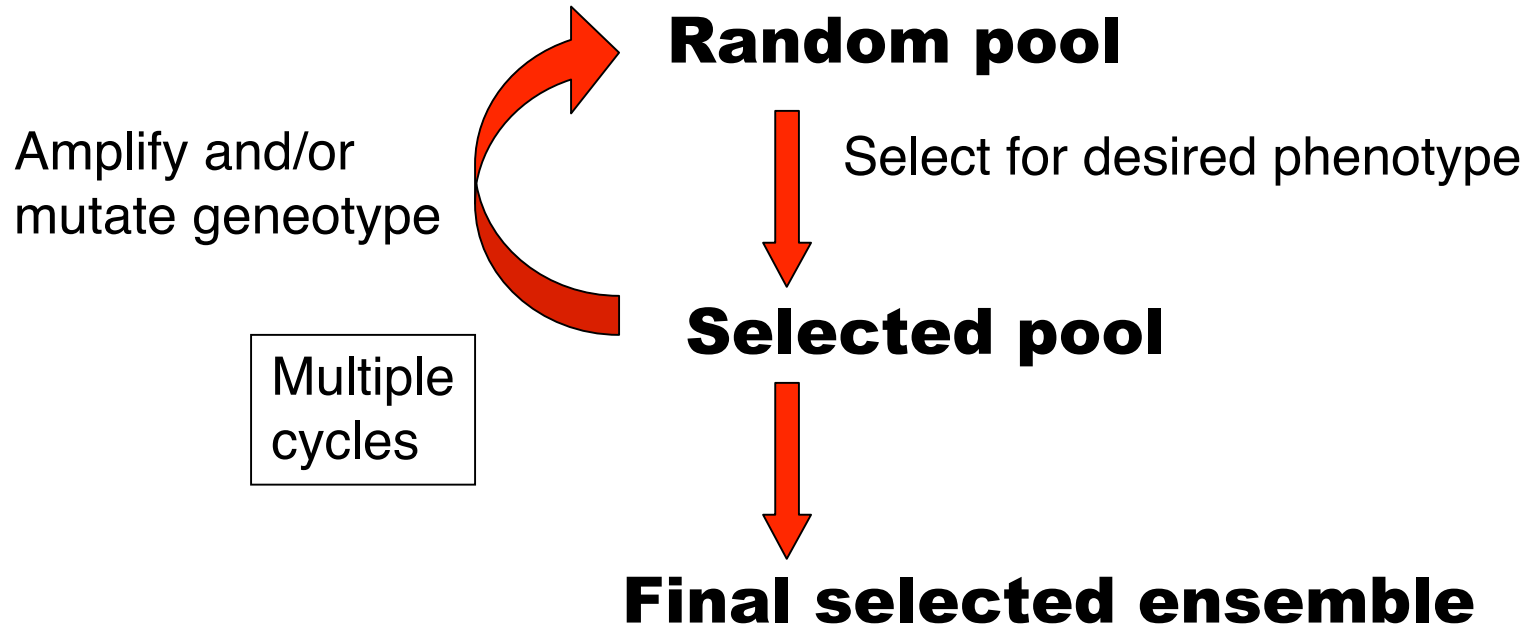


```

50      60      70      80      90      100     110     120
AAAGCGTACGAACTAAGTGATAAGGAAATTCAGATTAAGCGGAGCGGGATTCCGCACGTTGCGAGGGTTGCCCTTGG
130     140     150     160     170     180     190     200
CGAUCACTGTCTCCTCTCACTCTGTTCAAAAGCCGATTGCTGAACGTGTAAAACGCCATCACAAATATGTGCCCGIACGGCACC
210     220     230     240     250     260     270
GAGAAAAGCATAGGGTACGTCGGTGGAGATGTATAGTCTTAGGGTGAGGCTGGIATGACCGGTAACGGCTC
    
```

Fig. 9. Sequence of one of the isolated ribozymes. Members of pool 10 DNA were cloned (TA Cloning, Invitrogen) and sequenced. The sequence of the central 233 nucleotides of clone 4 is shown. Sequences of the 5' constant region (bases 1 to 42) and the 3' constant region (bases 276 to 295) are described in (29). Sty I and Ban I restriction sites used in pool construction are underlined. The 10 bases that differ from the consensus sequence of the dominant pool 10 sequence family are also underlined. Consensus bases at these positions are 56A, 63A, 90A, 94T, 96T, 131C, 188A, 195A, 217A, and 258A.

In vitro evolution of nucleic acids.



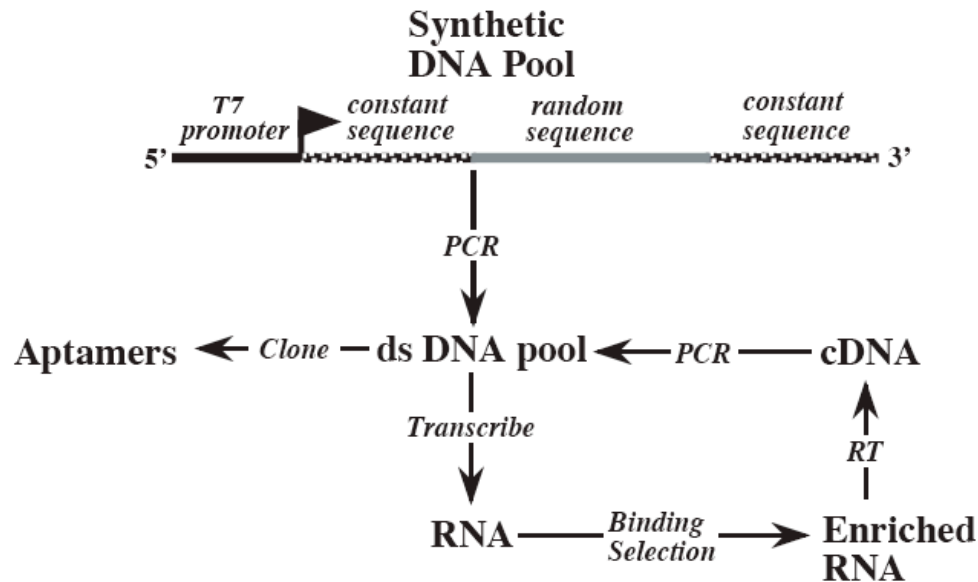
IN VITRO SELECTION OF FUNCTIONAL NUCLEIC ACIDS

David S. Wilson and Jack W. Szostak

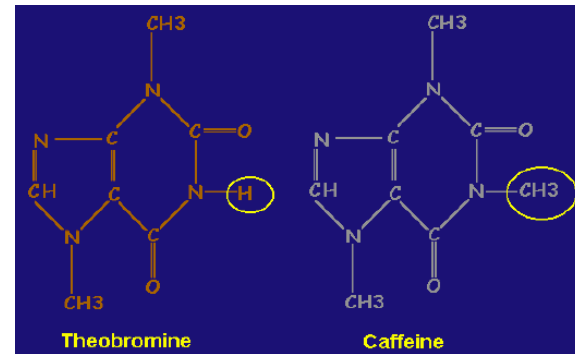
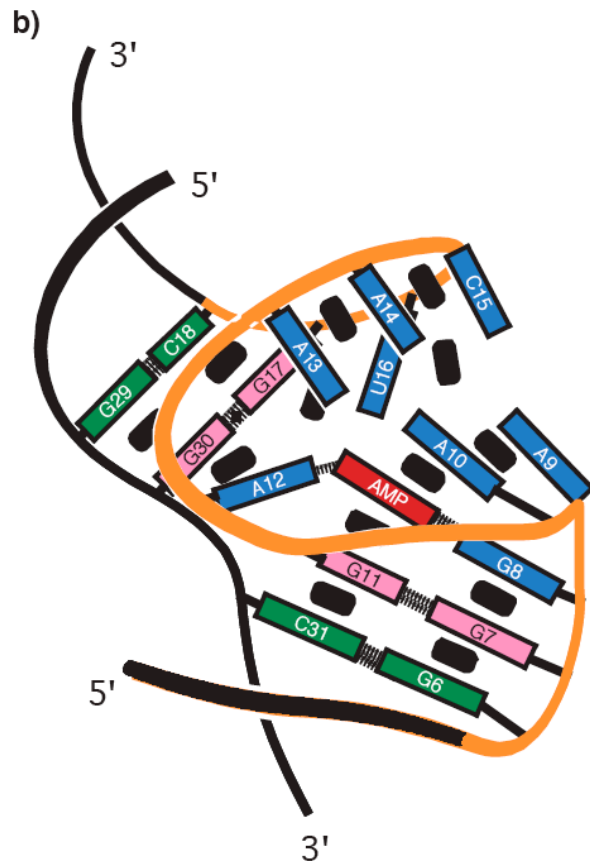
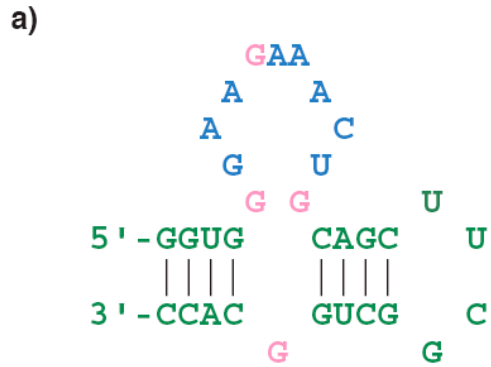
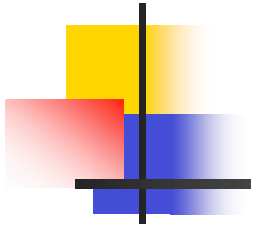
*Howard Hughes Medical Institute and Department of Molecular Biology,
Massachusetts General Hospital, Boston, Massachusetts 02114-2696;*

Annu. Rev. Biochem. 1999. 68:611-647

- In vitro selection requires linking of genotype and phenotype.
- Binding targets: simple ions, small molecules, peptides, proteins, organelles, and cells.



AMP binding aptamer



- Selectivity: theophylline aptamer shows 10,000-fold decrease in binding to caffeine which differs by one additional methyl group.

TABLE 1 Aptamers for small molecules

| Target | Estimated K_D (μM) | Target | Estimated K_D (μM) |
|--------------------------------|-----------------------------------|----------------------------------|-----------------------------------|
| Nucleotides and nucleobases | | Antibiotics | |
| ATP/adenosine | 1 | Tobramycin (aminoglycoside) | 0.0008 |
| ATP/adenosine (DNA) | 6 | Neomycin (aminoglycoside) | 0.1 |
| Guanosine | 32 | Lividomycin (aminoglycoside) | <0.2 |
| Guanine/xanthine | 1.8 | Kanamycin (aminoglycoside) | <0.2 |
| 7-Methyl-GTP | ~0.5 | Streptomycin (aminocyclitol) | ~1 |
| Theophylline | 0.11 | Viomycin (basic peptide) | 12 |
| Amino acids | | Chloramphenicol (small, neutral) | 2.1 |
| Arginine | 0.33 | Transition state analogs | |
| Citrulline | 62 | Diels-Alder reaction | 3,500 |
| Valine | 12,000 | Bridged biphenyl isomerization | 542 |
| Tryptophan | 18 | Other | |
| Cofactors | | Dopamine | 2.8 |
| Cyanocobalamin | 0.09 | Peptide (substance P) | 0.19 |
| N-methylmesoporphyrin IX | ~14 | Divalent metals | ~1 |
| N-methylmesoporphyrin IV (DNA) | ~0.5 | | |
| Flavin | 0.5 | | |
| NAD | 2.5 | | |
| RMP-biotin | 2 | | |

In vitro selection and directed evolution of peptides and proteins

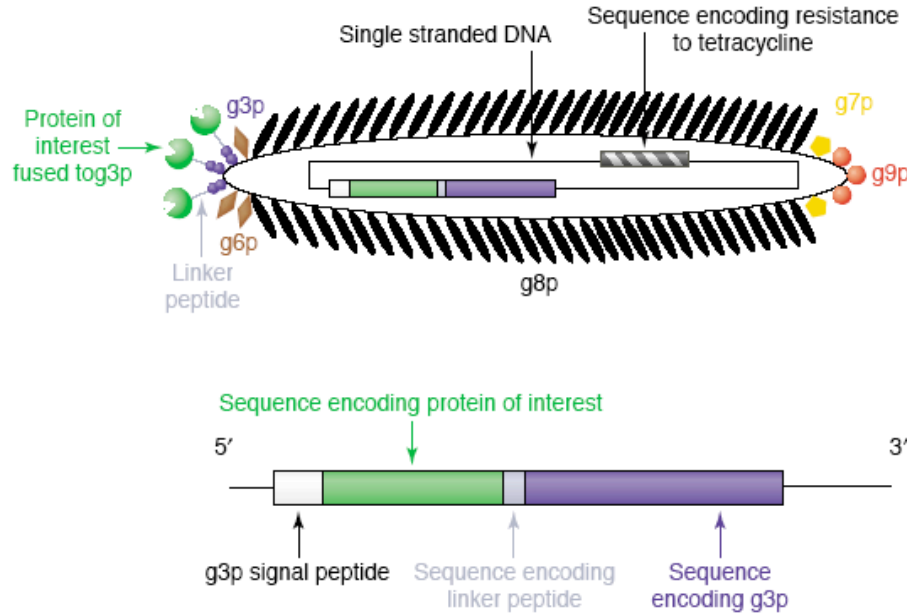
- Goal: find protein/peptide with desired function (binding, catalyst, stability, etc.)
- *In vivo* vs *In vitro* selection.
- Rational design vs. Library methods.
- Combinatorial peptide libraries.
 - Geysen. Discontinuous epitope mapping. Solid phase peptide synthesis. Birth of combinatorial chemistry.
- Phage display.
- mRNA fusion. Ribosome stalling.
- Antibody engineering and evolution.
- Primerless PCR. DNA shuffling. Sexual PCR.

Searching for Peptide Ligands with an Epitope Library

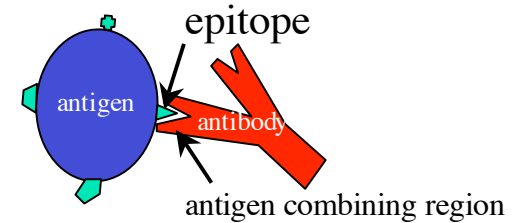
JAMIE K. SCOTT AND GEORGE P. SMITH*

Science, New Series, Vol. 249, No. 4967 (Jul. 27, 1990), 386-390.

Science, New Series, Vol. 228, No. 4705 (Jun. 14, 1985), 1315-1317.



Filamentous bacteriophage (M13, fd)



Cloning into p3 (pIII) coat protein

A fUSE5 RF Sfi I Sfi I
 5' -CTATTCTCACTCGGCCGACGGGGCTGGCCTCTGGGGCCGAAACTGTTGAA-3'
 3' -GATAAGAGTGAGCCGGCTGCACCGGACCGGAGACCCCGGCTTTGACAACCT-5'

B Degenerate Bgl I fragment
 GGGCT(NNK)₆GGGCCGCTG
 TGCCCGA(NNM)₆CCCCGGC

C Ligation product
 -CTATTCTCACTCGGCCGACGGGGCT(NNK)₆GGGCCGCTGGGGCCGAAACTGTTGAA-
 -GATAAGAGTGAGCCGGCTGCACCGA(NNM)₆CCCCGGCTACCCCGGCTTTGACAACCT-

D Recombinant pIII
 NH₂-A[DGA]₆[GAAGA]ETVE-

NNK codons: N=ACTG, K=GT.
 Encodes 32 triples, all 20 amino acids and only one stop codon.

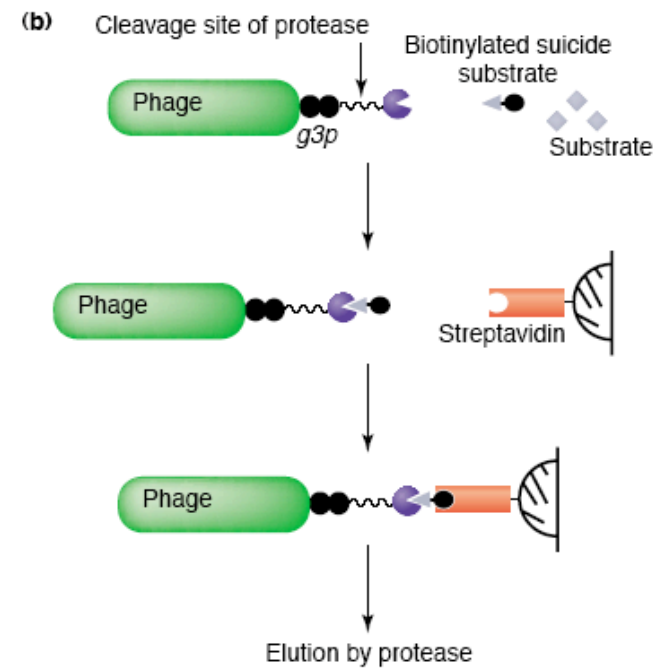
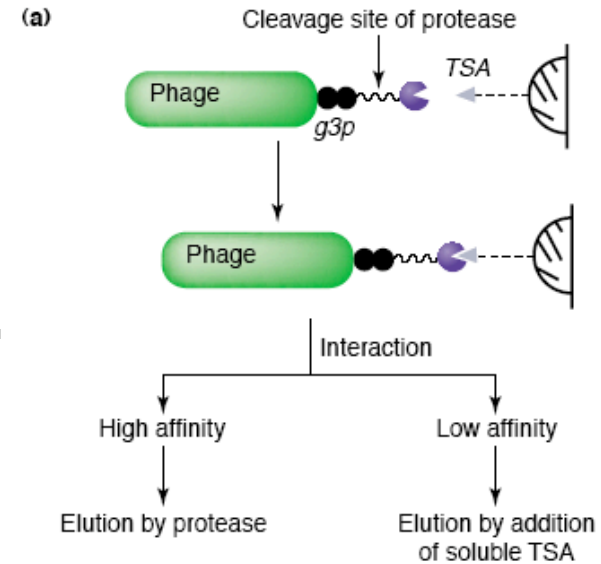
- 64 million possible hexapeptides
- Library contained 1.3×10^{14} phage from 2×10^8 clones

| Displayed peptides | | Number of clones isolated with | | Binding (OD $\times 10^3$) | | | |
|-------------------------------------|----------|--------------------------------|--------|-----------------------------|-----|--------|-----|
| | | | | MAb M33 | | MAb A2 | |
| No. | Sequence | MAb M33 | MAb A2 | Fab | IgG | Fab | IgG |
| MHr | DFLEKI | | | 72 | 352 | 136 | 235 |
| <i>Third round with 0.1 nM MAb</i> | | | | | | | |
| 1 | ----WL* | 16 | | 203 | 551 | 229 | 233 |
| 2 | ----ML | 1 | 2 | 92 | 558 | 269 | 236 |
| 3 | ---AWL | | 14 | 14 | 242 | 139 | 273 |
| <i>Second round with 0.1 nM MAb</i> | | | | | | | |
| 4 | ----R- | 1 | | 94 | 318 | 118 | 290 |
| 5 | CRFVWC | 2 | | 65 | 331 | -4 | -5 |
| 6 | CE---C | 1 | | 18 | 294 | -1 | 123 |
| 7 | CR---C | 1 | | 21 | 205 | 4 | 127 |
| 8 | --M-WL* | 1 | | 35 | 288 | 1 | 125 |
| 9 | ---VQL† | 1 | | 5 | 127 | 23 | 147 |
| 10 | ---AIV† | | 4 | 15 | 43 | 97 | 142 |
| 11 | ----Y- | | 2 | 67 | 157 | 9 | 253 |
| 12 | ----IL | | 1 | 100 | 431 | 159 | 308 |
| 13 | ----IV | | 1 | 37 | 168 | 195 | 293 |
| <i>Second round with 10 nM MAb</i> | | | | | | | |
| 14 | ----QL | 1 | | | | | |
| 15 | ----HF- | 1 | | 6 | 108 | -3 | -2 |
| 16 | AWERRG | 1 | | 4 | 8 | -3 | 9 |
| 17 | --F-I- | | 1 | 29 | 244 | 77 | 224 |
| 18 | ---MLV | | 1 | 3 | 18 | 17 | 50 |
| 19 | Q-VFCW | | 1 | 3 | 16 | -5 | 28 |

*Four clones with the peptide 1 sequence and one with the peptide 8 sequence were also isolated from the second round of AP with 10 nM MAb M33. †One clone each with the peptide 9 and 10 sequences were also isolated from the second round of AP with 10 nM MAb A2.

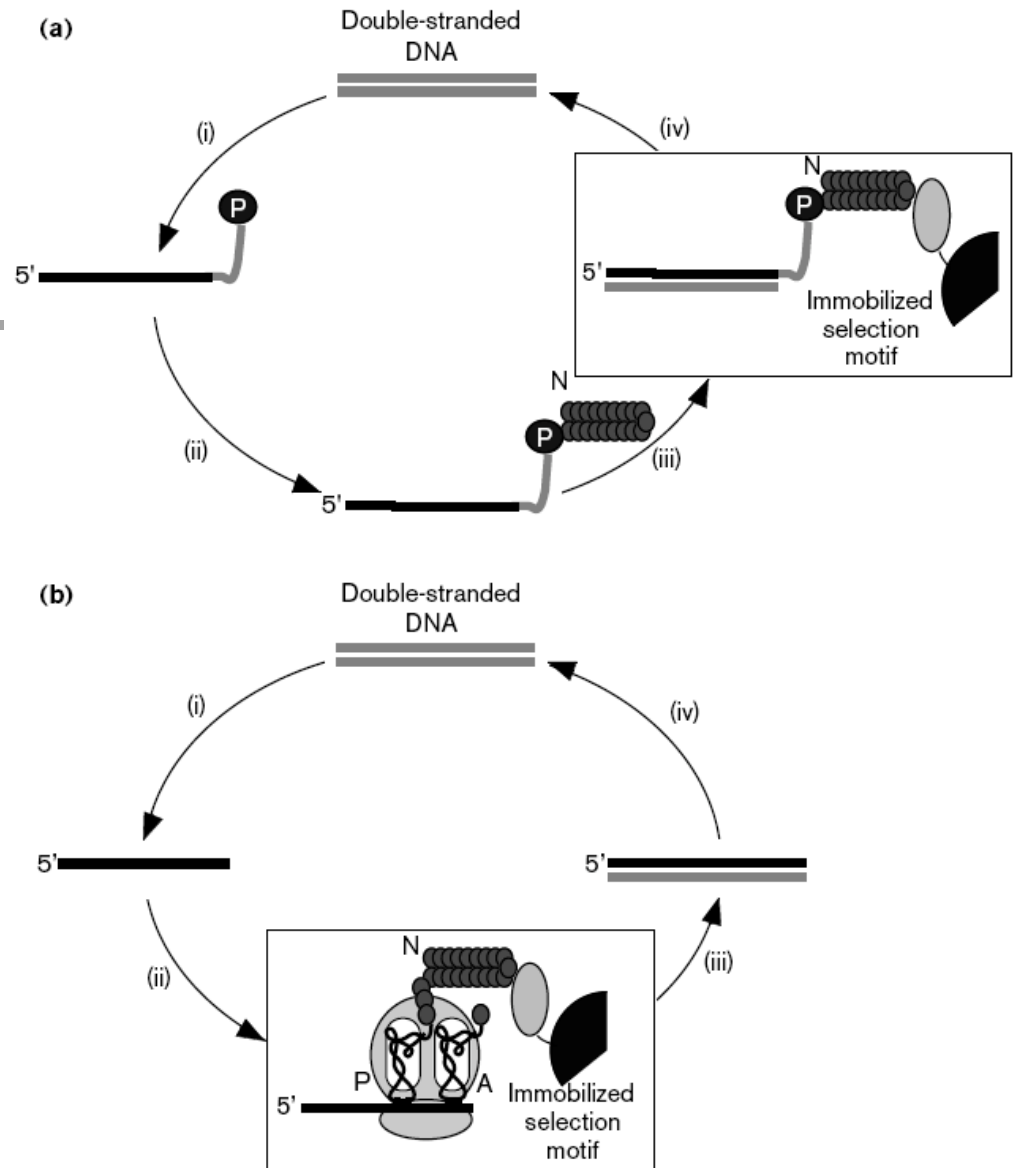
Phage display

- Enzyme selection.
- Note: hidden *in vivo* selection too...

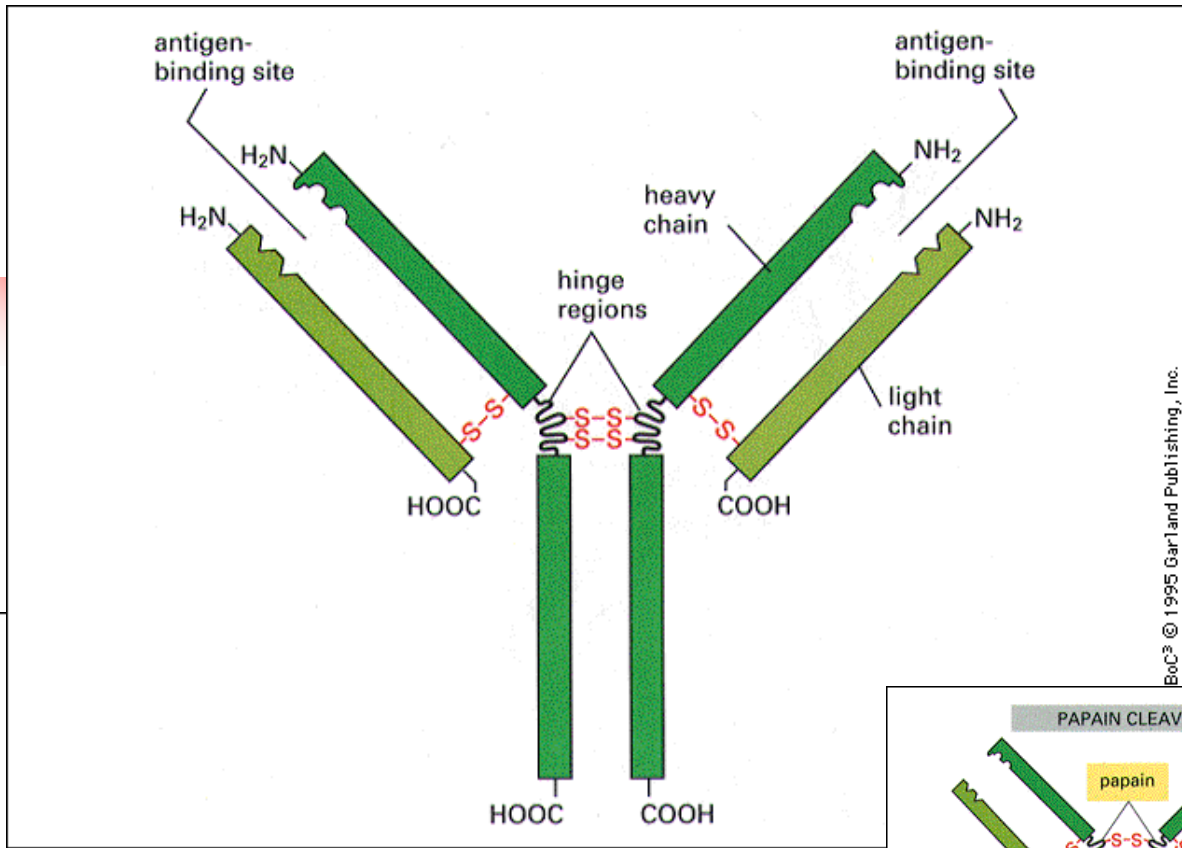




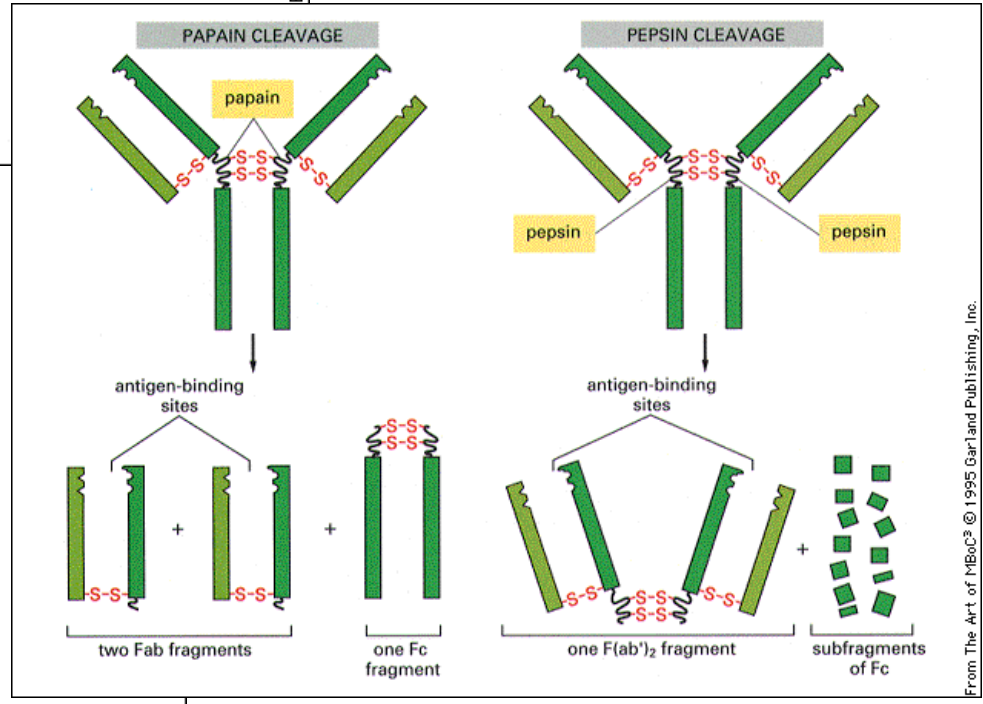
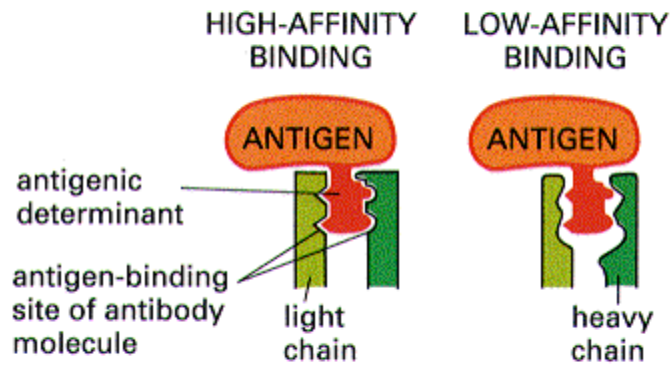
- mRNA-protein fusion
- Ribosome display
- Other. Cro?



Current Opinion in Chemical Biology

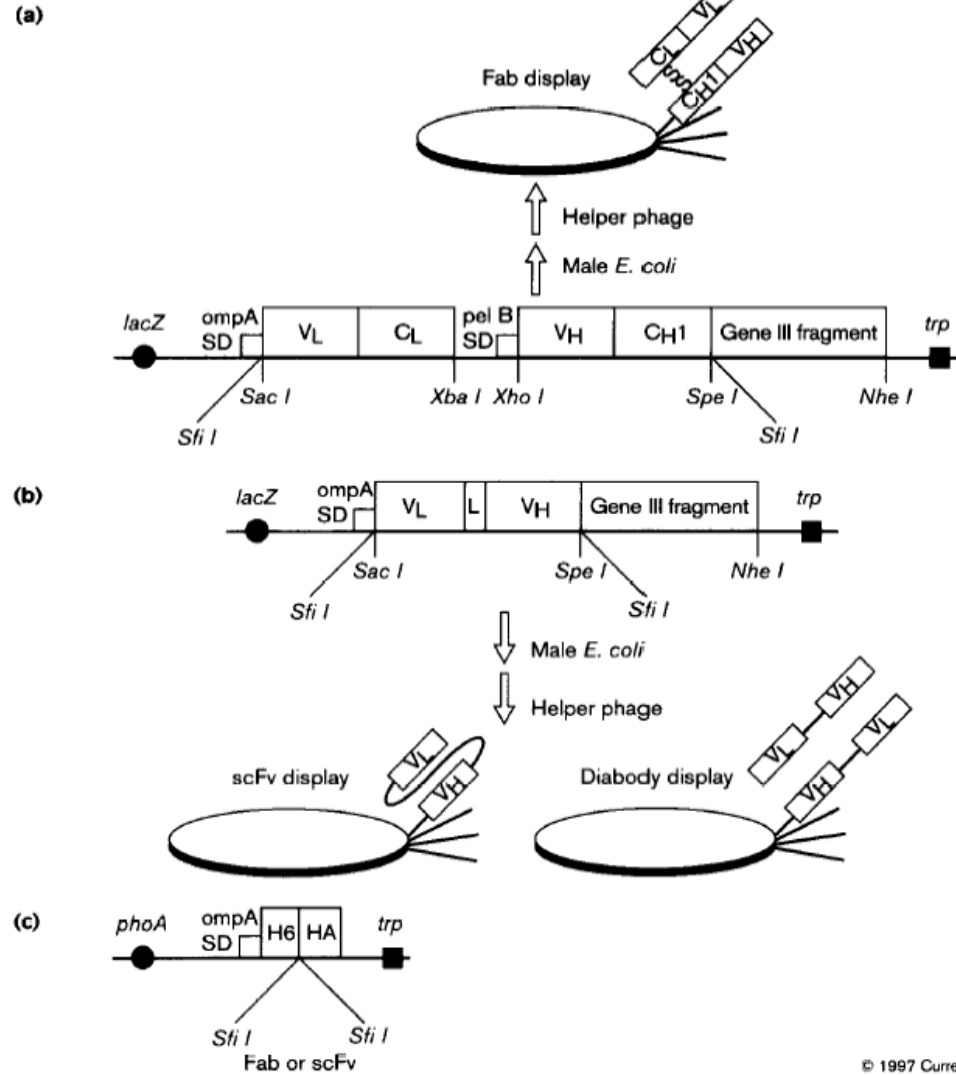
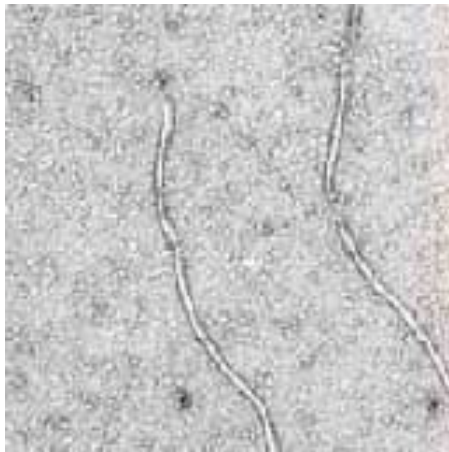
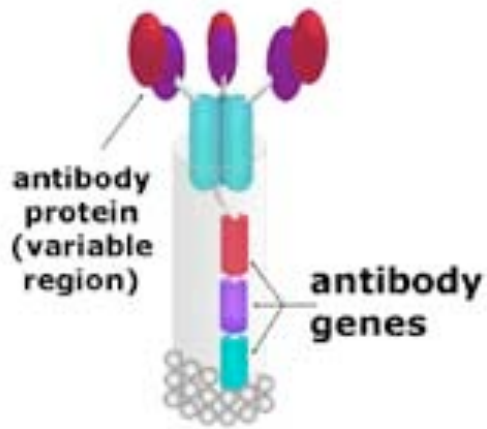


BoC³ © 1995 Garland Publishing, Inc.



From The Art of MBoC³ © 1995 Garland Publishing, Inc.

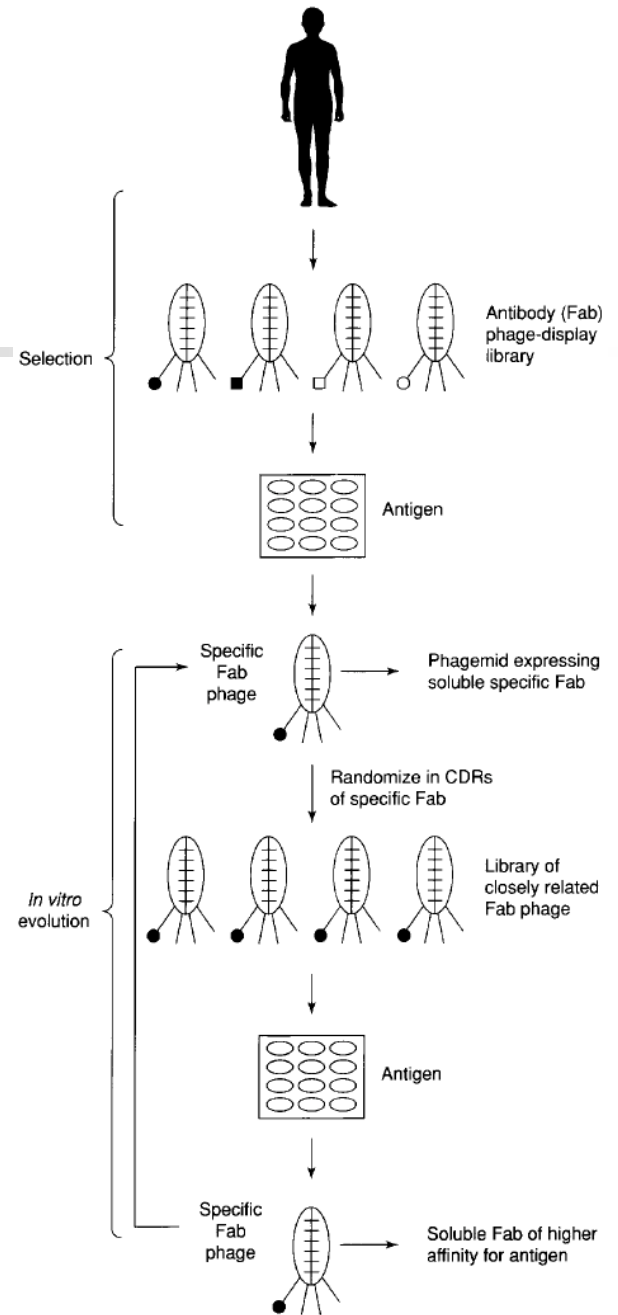
Phage display of Ab libraries



© 1997 Current Opinion

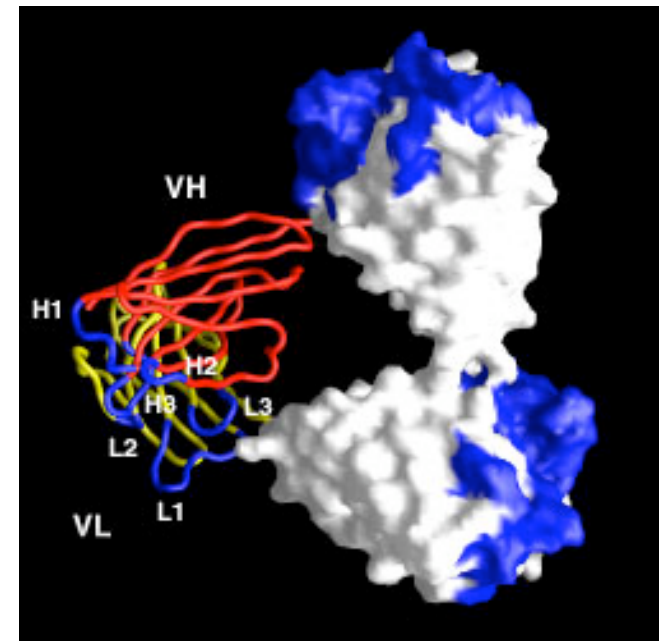
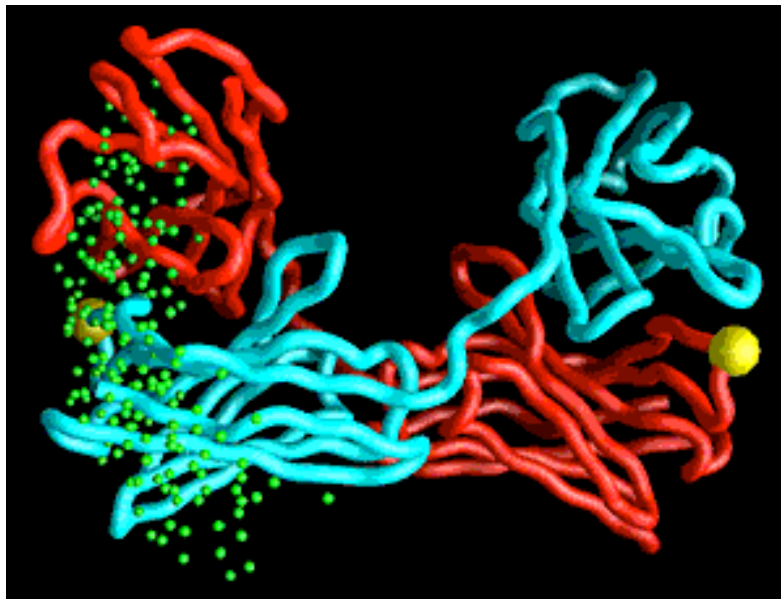
Artificial immune maturation

- Gene library from human, animal, or synthetic source.
- Maturation:
 - Saturation mutagenesis of CDRs.
 - Chain shuffling.
 - Growth in mutagenic *E. coli* strains.



Diabodies and triabodies

- In vitro selection/evolution of bifunctional antibody fragments.
- Universal protein-based adapter/address system.



DNA shuffling by random fragmentation and reassembly: *In vitro* recombination for molecular evolution

WILLEM P. C. STEMMER

Affymax Research Institute, 4001 Miranda Avenue, Palo Alto, CA 94304

Proc. Natl. Acad. Sci. USA

Vol. 91, pp. 10747–10751, October 1994

<http://www.maxygen.com/science-pub.php>

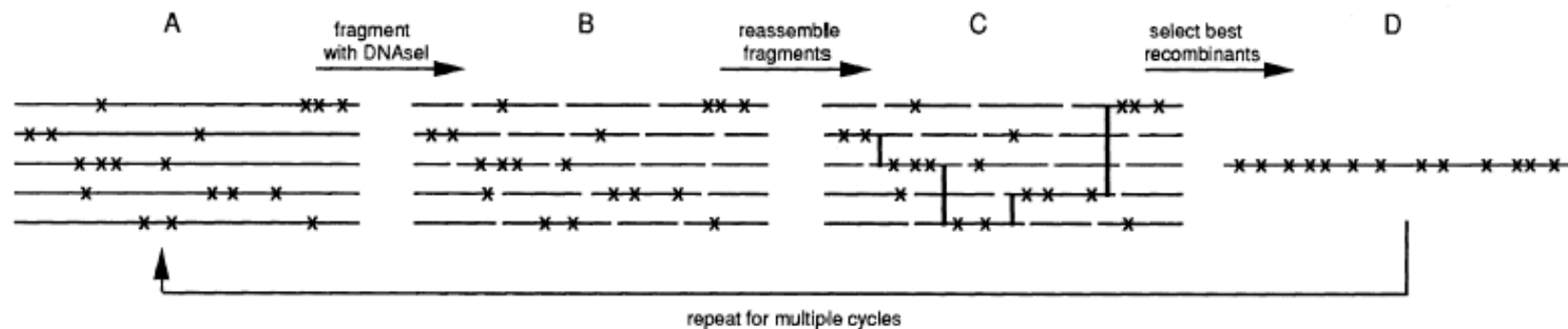


FIG. 1. (A) A pool of homologous genes with different point mutations is fragmented with DNase I. (B) For simplicity, all mutations shown are considered beneficial and additive. (C) Reassembly of the random fragments into full-length genes results in frequent template switching and recombination. A recombinant gene containing the four crossovers (thick lines) can be selected from the library of recombinants based on its improved function. (D) Selected pool of improved recombinants provides the starting point for another round of mutation and recombination. The recombination process alone causes a low level of point mutations but, if desired, additional mutations could be introduced by error-prone PCR or UV mutagenesis of the pool of genes.

- Gene reassembly
- Whole plasmid reassembly

Table 1. Mutations introduced by mutagenic shuffling

| Transition | Frequency | Transversion | Frequency |
|------------|-----------|--------------|-----------|
| G → A | 6 | A → T | 1 |
| A → G | 4 | A → C | 2 |
| C → T | 7 | C → A | 1 |
| T → C | 3 | C → G | 0 |
| | | G → C | 3 |
| | | G → T | 2 |
| | | T → A | 1 |
| | | T → G | 2 |

A total of 4437 bases of shuffled *lacZ* DNA were sequenced. The mutation rate was 0.7%; 11/12 types of base substitutions were found, but there were no frameshifts.

DNA shuffling of a family of genes from diverse species accelerates directed evolution

NATURE | VOL 391 | 15 JANUARY 1998

Andreas Cramer, Sun-Ai Raillard, Ericka Bermudez
& Willem P. C. Stemmer

Maxygen Inc., 3410 Central Expressway, Santa Clara, California 95051, USA

- Can natural diversity accelerate the evolution process?
- Goal: obtain moxalactamase activity from four cephalosporinase genes. DNA shuffling within genes or between genes...

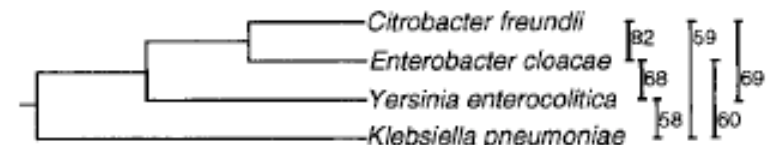


Figure 1 Phylogenetic tree of the four cephalosporinase genes. The numbers on the vertical bars indicate the percentage of DNA sequence similarity.

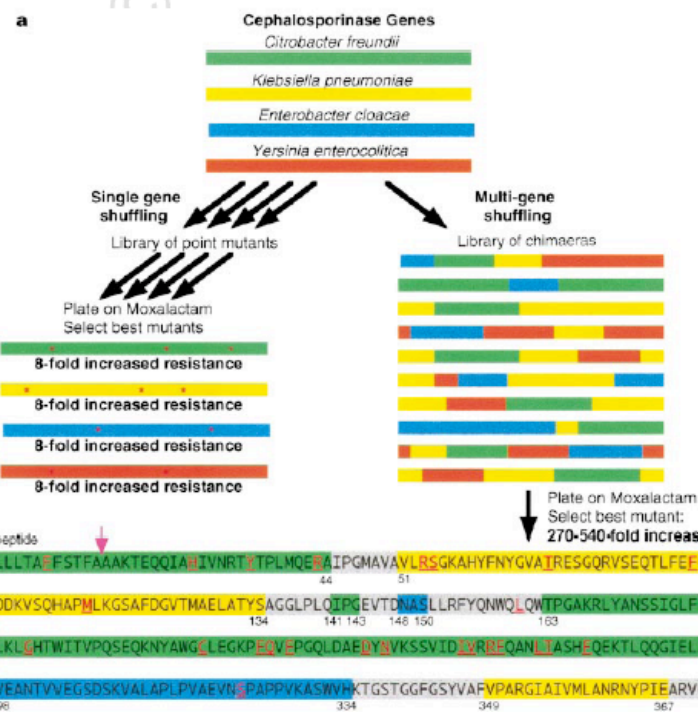
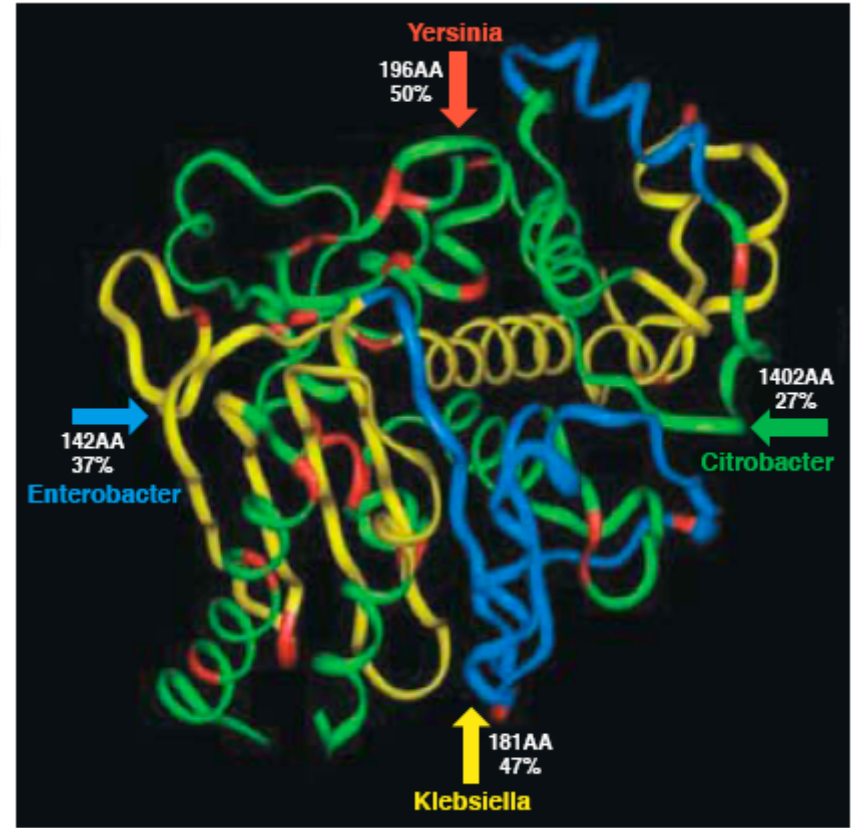


Figure 2 a, Comparison of single sequence shuffling versus sequence family shuffling. **b**, Sequence of chimaeric mutant A obtained by family shuffling. The segments derived from *Enterobacter* are shown in blue, those from *Klebsiella* are shown in yellow, and those from *Citrobacter* are shown in green. The grey segments are where the crossovers have taken place. Because of DNA homology in the grey segments, the exact location of the crossover cannot be determined more exactly. The amino-acid point mutations are shown with underlined red letters. The numbers at the beginning and end of each segment are the numbers from the Genbank protein files of the wild-type enzymes and differ from those used for the *Enterobacter cloacae* enzyme¹⁴.



Stemmer

NATURE | VOL 391 | 15 JANUARY 1998

3/29/06

LaBean COMP

- Can natural diversity accelerate the evolution process?
- Goal: obtain moxalactamase activity from four cephalosporinase genes. DNA shuffling within genes or between genes...
- One cycle: ~8-fold improvements from separately evolved genes.
- One cycle: 270- to 540-fold improvement from the four genes shuffled together.
- Best clone contained 8 segments from 3 of the 4 genes & 33 amino-acid point mutations.

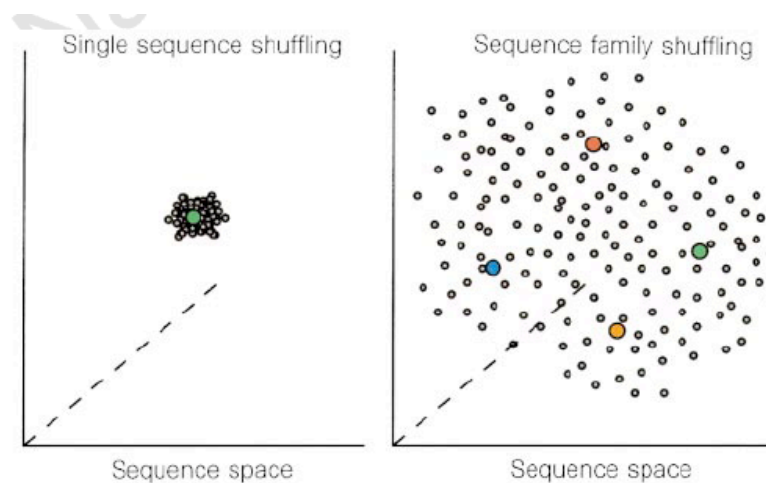


Figure 4 Searching sequence space by family shuffling versus by single sequence shuffling. Single sequence shuffling yields clones with a few point mutations and the library members are typically 97–99% identical. Family shuffling causes sequence block exchange which yields chimaeras that have greater sequence divergence. At equal library size, the increased sequence diversity of the chimaeric library results in sparse sampling of a much greater area of sequence space, allowing more promising areas to be found and subsequently explored at increased sampling density.

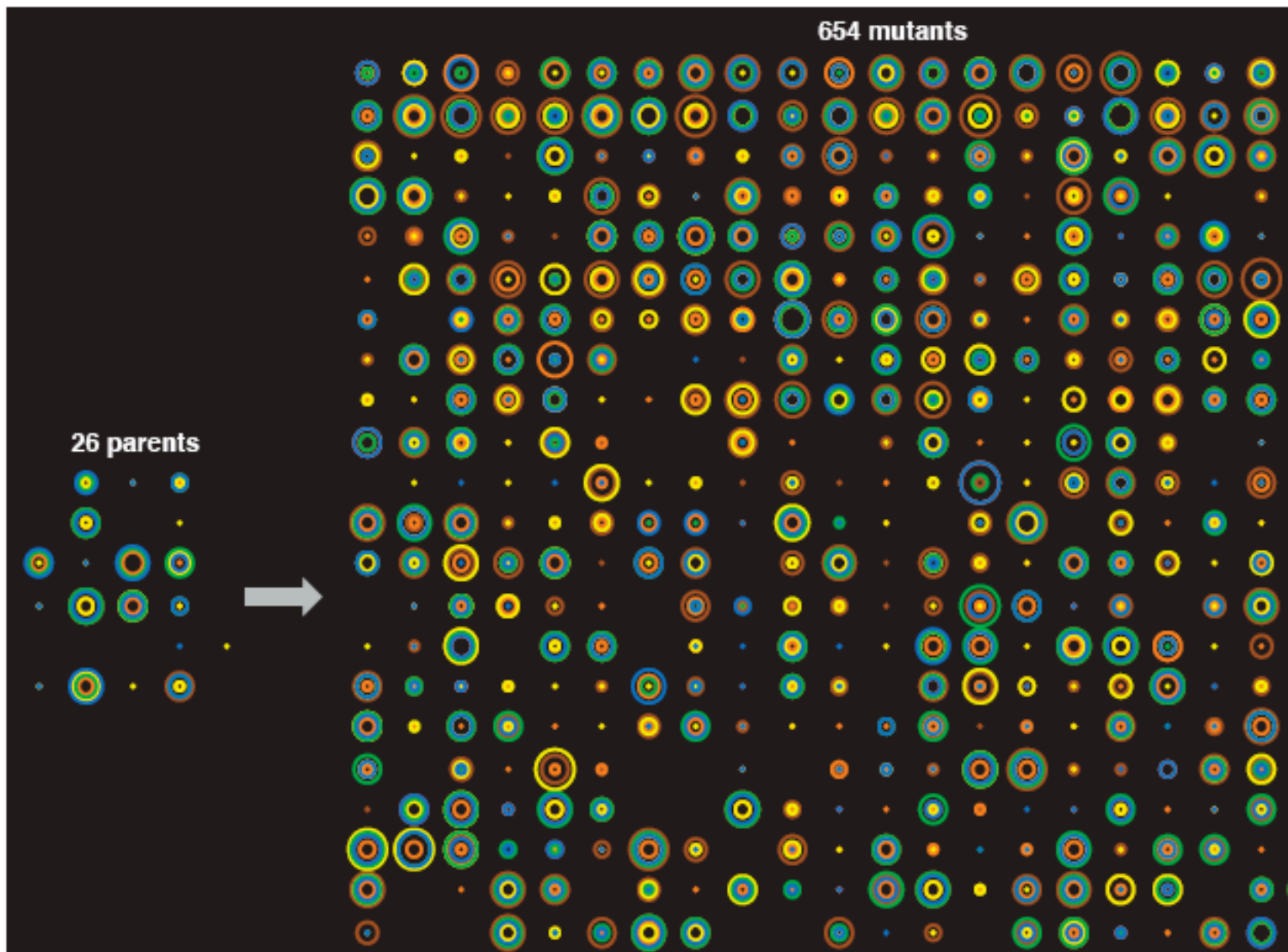


Figure 6. DNA family breeding of the subtilisin gene illustrates the potential for rapid improvement in protein function. Subtilisin is a protein-degrading enzyme used in laundry detergent and the most highly engineered enzyme in existence. Twenty-six subtilisin genes from various *Bacillus* microbes were shuffled to yield 654 progeny that were screened for enzyme activity at five commercially relevant conditions. Each clone is shown as a set of concentric circles, with the size of the circle indicating the activity of the enzyme and each assay condition represented by a different color. Several progeny showed simultaneous improvement in multiple properties over the best parental sequences.

3/29/06

LaBean COMPSCI 296.5

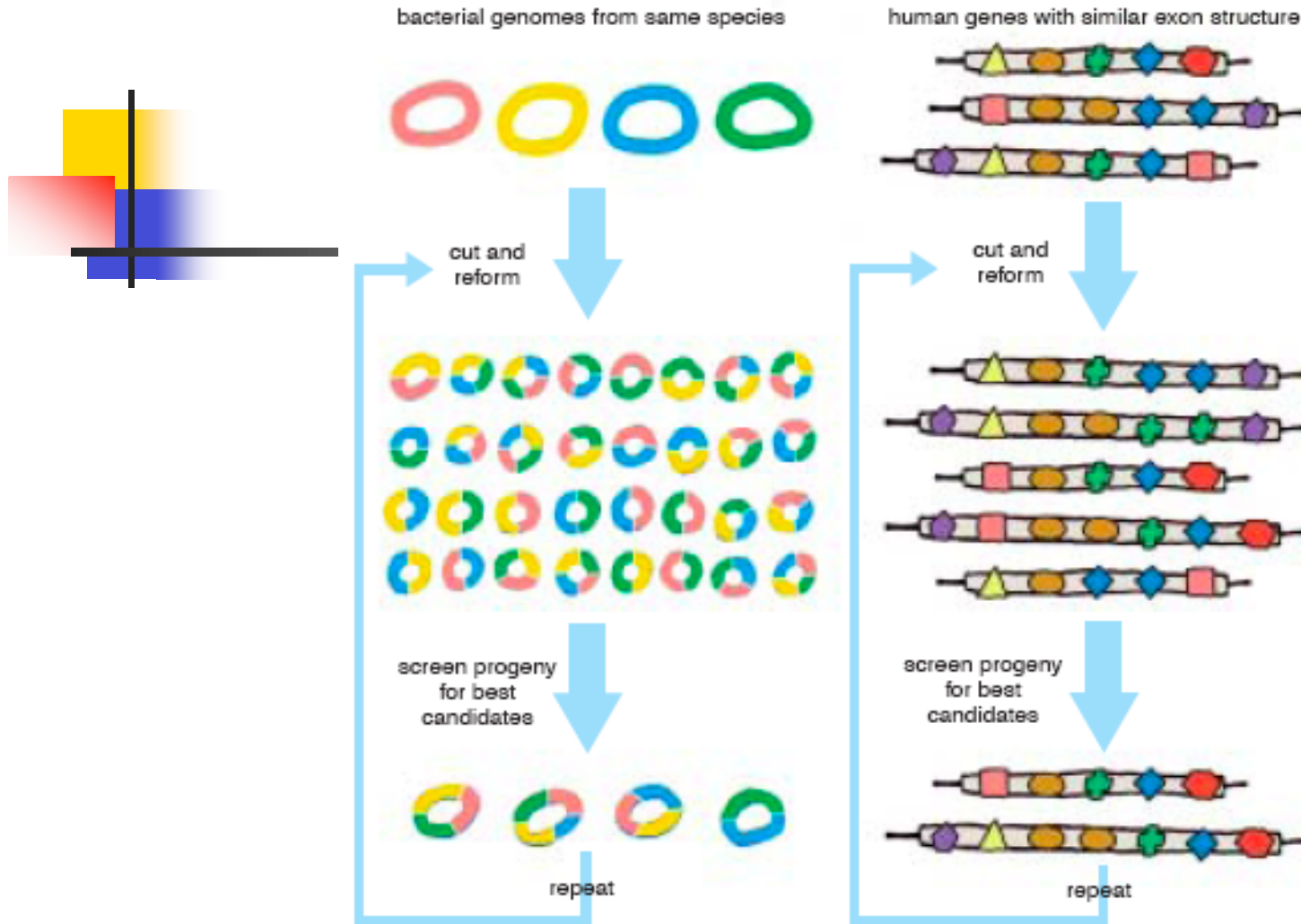


Figure 7. Genome shuffling (*left*) and exon shuffling (*right*) are two other applications of the DNA breeding technique. Genome shuffling is modeled after the natural evolution of prokaryotic organisms, whereas exon shuffling mimics eukaryotic protein evolution. In both cases the progeny are more likely to have useful properties because the breeding step starts with “proven diversity”—natural selection having already removed most deleterious point mutants.

Belcher

(2000) *Nature* **405**, 665-668

Selection of peptides with semiconductor binding specificity for directed nanocrystal assembly

Sandra R. Whaley*, D. S. English*, Evelyn L. Hu†, Paul F. Barbara*‡ & Angela M. Belcher*‡

| | | | | | | | | | | | | | | |
|-------|---|---|---|---|---|---|---|---|---|---|---|---|---|---|
| G13-5 | | V | T | S | P | D | S | T | T | G | A | M | A | |
| G12-5 | | A | A | S | P | T | Q | S | M | S | Q | A | P | |
| G12-3 | | A | Q | N | P | S | D | N | N | T | H | T | H | |
| G1-4 | A | S | S | S | R | S | H | F | G | Q | T | D | | |
| G12-4 | | W | A | H | A | P | Q | L | A | S | S | S | T | |
| G14-3 | A | R | Y | D | L | S | I | P | S | S | E | S | | |
| G7-4 | | T | P | P | R | P | I | Q | Y | N | H | T | S | |
| G15-5 | | S | S | L | Q | L | P | E | N | S | F | P | H | |
| G14-4 | | | G | T | L | A | N | Q | Q | I | F | L | S | S |
| G11-3 | | H | G | N | P | L | P | M | T | P | F | P | G | |
| G1-3 | | R | L | E | L | A | I | P | L | Q | G | S | G | |

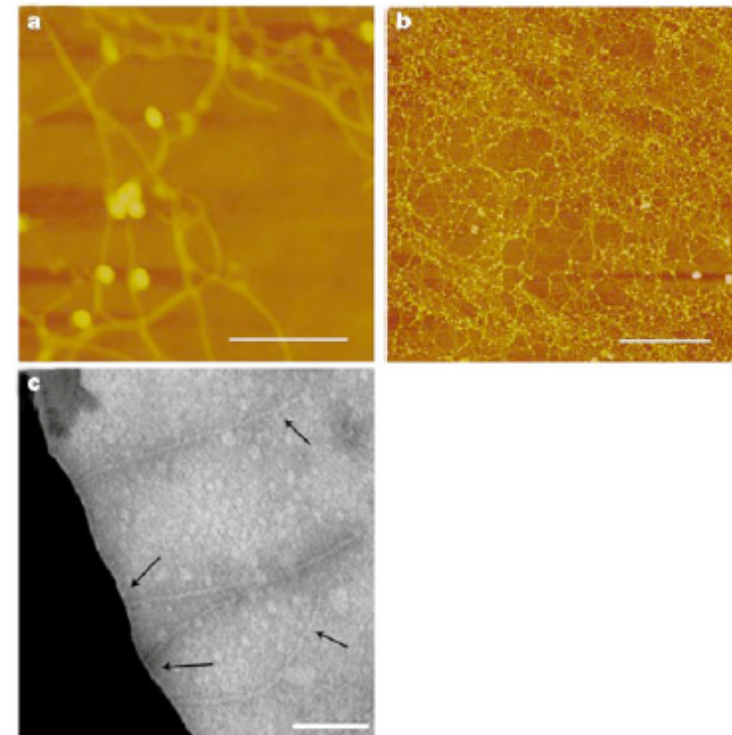


Figure 3 AFM and TEM analysis of peptide–semiconductor recognition. **a, b**, AFM images of G1-3 phage bound to an InP(100) substrate. **a**, Individual phage and their attached Au nanoparticles. Scale bar, 250 nm. **b**, Image showing the uniformity of phage coverage on the InP surface. Scale bar, 2.5 μm . **c**, TEM image of G1-3 phage recognition of GaAs. Individual phage particles are indicated with arrows. Scale bar, 500 nm.

Belcher

(2000) *Nature* **405**, 665-668

- GaAs (100), GaAs(111), InP, GaN, ZnS, CdS, Fe₃O₄, CaCO₃, etc.

